GEORGIA INSTITUTE OF TECHNOLOGY — OFFICE OF CONTRACT ADMINISTRATION

PROJECT ADMINISTRATION DATA SHEET

[X] ORIGINAL [ ] REVISION NO. ______

Project No. E-16-602 (R6045-0A0) GTRC/~~GIT~~ DATE 10 / 9 / 85

Project Director: W. C. Strahle School/~~Lab~~ AE

Sponsor: National Science Foundation

Type Agreement: Grant No. CBT-8414906

Award Period: From 10/1/85 To ~~3/31/88~~ 3/31/89 (Performance) 6/31/87 (Reports)

Sponsor Amount:

	This Change	Total to Date
Estimated:	$	$ 187,209
Funded:	$	$ 41,949

Cost Sharing Amount: $ 9,711 Cost Sharing No: E-16-378

Title: Effect of Pressure in Turbulent Reacting Flows

ADMINISTRATIVE DATA

OCA Contact John B. Schonk x-4820

1) Sponsor Technical Contact:

Win Aung
National Science Foundation
ENG/CBT
Washington, D. C. 20550
(202) 357-9606

2) Sponsor Admin/Contractual Matters:

Altie H. Metcalf
National Science Foundation
DGC/ENG
Washington, D.C. 20550
(202) 357-9602

Defense Priority Rating: N/A

Military Security Classification: N/A
(or) Company/Industrial Proprietary: N/A

RESTRICTIONS

See Attached NSF Supplemental Information Sheet for Additional Requirements.

Travel: Foreign travel must have prior approval – Contact OCA in each case. Domestic travel requires sponsor approval where total will exceed greater of $500 or 125% of approved proposal budget category.

Equipment: Title vests with GIT

COMMENTS:

* Includes 6 month unfunded flexibility period.

No funds may be expended after 3/31/87.

COPIES TO:

SPONSOR'S I. D. NO. 02.102.000.85.124

Project Director
Research Administrative Network
Research Property Management
Accounting
Procurement/GTRI Supply Services
Research Security Services
Reports Coordinator (OCA)
Research Communications (2)
GTRC
Library
Project File
Other A. Jones

FORM OCA 65:285

GEORGIA INSTITUTE OF TECHNOLOGY
OFFICE OF CONTRACT ADMINISTRATION

NOTICE OF PROJECT CLOSEOUT

Date 5/3/89

Project No. E-16-602 Center No. R6045-0A0

Project Director W. C. Strahle School/Lab AE

Sponsor National Science Foundation

Contract/Grant No. CBT-8414906 GTRC XX GIT ____

Prime Contract No. ____

Title Effects of Pressure in Turbulent Reacting Flows

Effective Completion Date 3/31/89 (Performance) 6/30/89 (Reports)

Closeout Actions Required:

- X None
- ___ Final Invoice or Copy of Last Invoice
- ___ Final Report of Inventions and/or Subcontracts
- ___ Government Property Inventory & Related Certificate
- ___ Classified Material Certificate
- ___ Release and Assignment
- ___ Other ____

Includes Subproject No(s). ____

Subproject Under Main Project No. ____

Continues Project No. ____ Continued by Project No. ____

Distribution:

- X Project Director
- X Administrative Network
- X Accounting
- X Procurement/GTRI Supply Services
- X Research Property Management
- ___ Research Security Services
- X Reports Coordinator (OCA)
- X GTRC
- X Project File
- X Contract Support Division (OCA)
- ___ Other ____

PROGRESS TO DATE

June 6, 1986

Grant No. CBT-8414906

The purpose of the program is to measure and model two elusive correlations which have given extreme trouble in the past in turbulent reacting flow calculations. These correlations occur between the pressure gradient and both the velocity fluctuations and species concentration fluctuations. The correlations appear in the following form in the theory of turbulent reacting flows:

$$C_{k\ell} \equiv \overline{v_k'' \, \partial p / \partial x_\ell}$$

$$D_\ell \equiv \overline{c_i'' \, \partial p / \partial x_\ell}$$

In the above, v_k is the velocity in the k^{th} direction, p is the pressure and c_i is the mass fraction of species i. The double prime superscript denotes a Favre, or mass weighted, fluctuation and the overbar indicates an ordinary time average. These correlations are exceptionally difficult to measure since they contain the fluctuating static pressure and require measurement of a gradient. They are equally difficult to model because of only scant experimental data available to guide the modelling work.

The experimental work to date has centered about a.) construction of a moveable premixed gas burner to allow a fixed laser with a moveable experiment for simple laser diagnostics, b.) training of a new graduate student in the use of the laser Rayleigh scattering system and dynamic Pitot tube measuring system and c.) initial cold flow experiments to remove or explain some inconsistencies between theory and experiment in the correlation between the pressure fluctuation and velocity fluctuation.

It has been decided to initially attempt to measure D_1 because it is a a vector, as opposed to $C_{k\ell}$ which is a second order tensor. The measurement requires a mass fraction measurement, which will be done by laser Rayleigh scattering on a premixed methane-air flame. The use of a dynamic Pitot tube for pressure measurement requires that a velocity measurement be simultaneously conducted. The velocity measurement will be made using laser velocimetry. The measuring systems are in place and the burner construction is complete.

The analytical work is being conducted by the Principal Investigator and consists of three elements. The first is to confirm that inconsistencies exist between some past experimental results and the line-integrated momentum equation in the correlation between pressure and velocity. In the process, a new theory for this correlation will emerge, and it will have the experimental backing as mentioned above. Secondly, a new form of a model for the pressure-strain correlation is being developed, which will hopefully reduce to past models in the incompressible limit and will conform to the experimental results of this program in reactive flows. Thirdly, the procedure developed in the second phase will be extended to model the mass fraction - pressure gradient correlation. Here, however, since there is no current experimental guidance, it will be necessary to wait for the initial experimental results of this program.

The program is proceeding as expected, and no difficulties other than those anticipated have arisen.

Current and Pending Support

	Agency	Title	Annual Rate	Period	ACAD (man mos.)	Summ (man mos.)	Location
Dr. Warren C. Strahle							
A. Current Support other than NSF Grant							
1.	ARO	Stagnating Turbulent Reacting Flows	$ 56,867	10/1/85-9/30/86	1.35	.45	Georgia Tech
2.	AFOSR	Heterogeneous Diffusion Flame Stabilization	$ 196,577 (2 PI's)	10/1/86-9/30/87	. 9	. 3	Georgia Tech
3.	ONR	Acoustic Response of Turbulent Reacting Recirculatory Flows	$ 98,000	4/1/86-3/31/87	1.35	.45	Georgia Tech
B. Proposals Pending							
1.	AFOSR	Universities Research Initiative in Turbulent Reactive Flows	$ 1,000,000 (7 PI's)	10/1/86-9/30/89	1.35	.45	Georgia Tech
C. Planned Proposals							
1.	ARO	Stagnating Turbulent Reacting Flows	$ 60,000	12/1/86-11/30/89	1.35	.45	Georgia Tech

PROGRESS TO DATE

June 2, 1987

Grant No. CBT-8414906

The purpose of the program is to measure and model two elusive correlations which have given extreme trouble in the past in turbulent reacting flow calculations. These correlations occur between the pressure gradient and both the velocity fluctuation and species concentration fluctuation. The correlations appear in the following form in the theory of turbulent reacting flows:

$$C_{k\ell} \equiv \overline{v_k'' \, \partial p/\partial x_\ell}$$

$$D_\ell \equiv \overline{c_i'' \, \partial p/\partial x_\ell}$$

In the above, v_k is the velocity in the k^{th} direction, p is the pressure and c_i is the mass fraction of species i. The double prime superscript denotes a Favre, or mass weighted, fluctuation and the overbar indicates an ordinary time average. These correlations are exceptionally difficult to measure since they contain the fluctuating static pressure and require measurement of a gradient. They are equally difficult to model because of only scant experimental data available to guide the modelling work.

The burner and flame being used for the experimental investigation are shown in the appended photograph. A methane-air flame is being used for minimal molecular weight effects in Rayleigh scattering measurement of gas density. Velocity is being measured in two components by a 5 watt argon-ion laser velocimeter. Pressure is being measured by a dynamic pitot guage, corrected for frequency response. Because gradients are involved in the above correlations an enormous number of one and two point correlations must be obtained with simultaneous measurements. Software development to treat the data has occupied much of the past year. Moreover, the Rayleigh measurement is contaminated by background radiation from the flame and special data reduction methods have had to be developed to remove this noise from the desired signal.

The Rayleigh scattering measurements to data have shown an interesting two-temperature structure to the flame. This structure, known as the Bray Moss Libby structure, was hoped for, because it can aid the data reduction process. It was necessary, however, to prove this structure before incorporating the fact in this data reduction scheme.

The analytical work is being conducted by the PI. Recently, a new model for the pressure-strain and pressure-scalar gradient has been generated. This model has been compared against some results of a prior NSF program and has been found promising. A full test of the model awaits the current experimental results, however. A new model for the pressure-velocity and pressure-scalar correlations is also currently under development and is being compared with some cold flow results. This model too is to be tested by the current experiment.

All facilities, diagnostics and software are now operational and experiments are being conducted. The program is proceeding as planned.

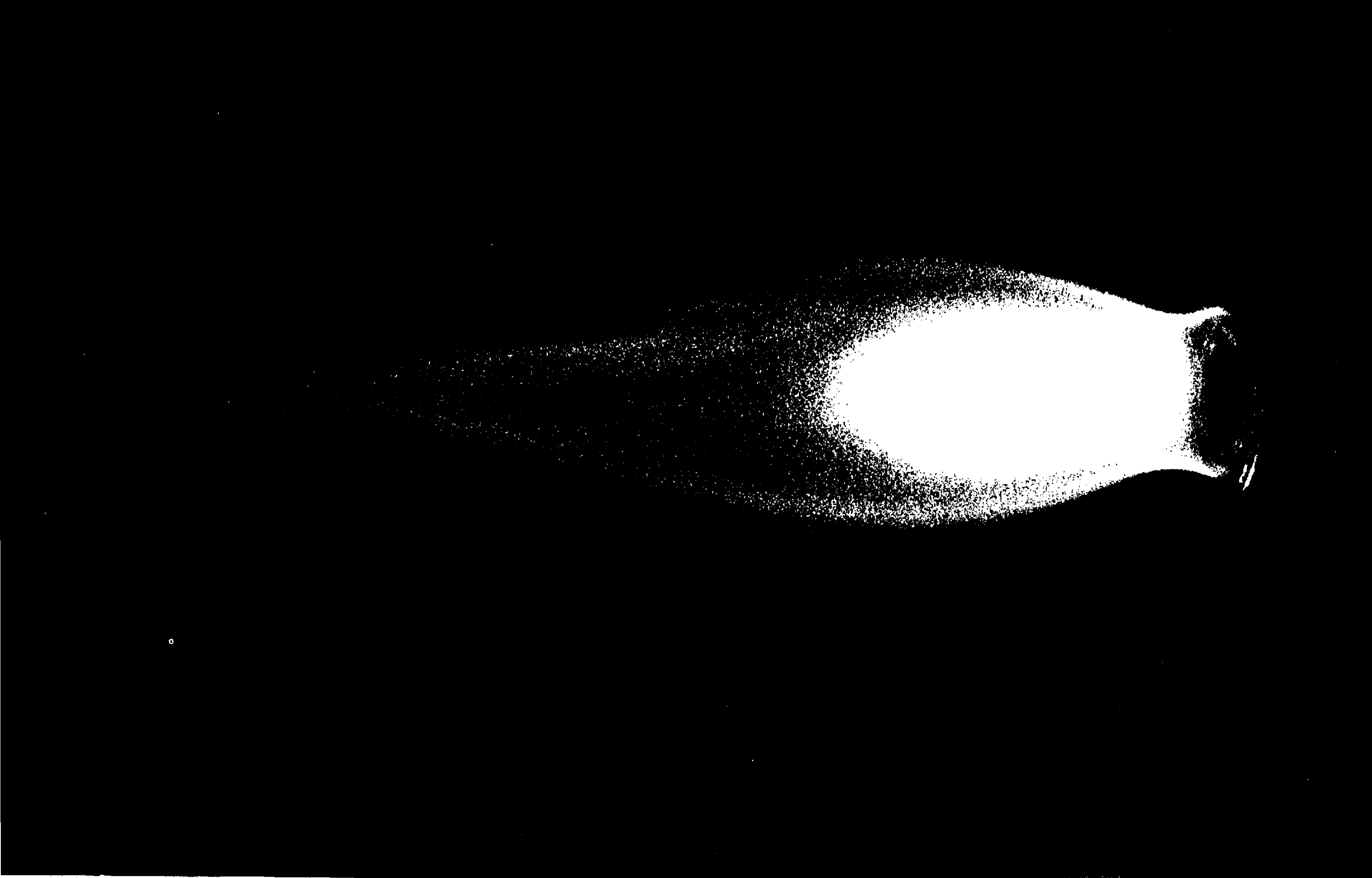

Current and Pending Support

	Agency	Title	Annual Rate	Period	ACAD (man mos.)	Summ (man mos.)	Location
Dr. Warren C. Strahle							
A. Current Support other than NSF Grant							
1.	ARO	Stagnating Turbulent Reacting Flows	56,867	10/1/86-9/30/87	1.35	.45	Georgia Tech
2.	AFOSR	Heterogeneous Diffusion Flame Stabilization	196,577 (2 PI's)	10/1/86-9/30/87	.9	.3	Georgia Tech
3.	ONR	Acoustic Response of Turbulent Reacting Recirculatory Flows	98,000	4/1/87-7/30/88	1.35	.45	Georgia Tech
B. Proposals Pending							
1.	AFOSR	Fractal Image Compression of Rayleigh, Raman, LIF, and LV Data in Turbulent Reacting Flows	153,965 (2 PI's)	10/1/87 9/30/90	1.8	.6	Georgia Tech
C. Planned Proposals							
1. None							

NATIONAL SCIENCE FOUNDATION
Washington, D.C. 20550

FINAL PROJECT REPORT
NSF FORM 98A

PLEASE READ INSTRUCTIONS ON REVERSE BEFORE COMPLETING

PART I—PROJECT IDENTIFICATION INFORMATION

1. Institution and Address	2. NSF Program	3. NSF Award Number
Georgia Institute of Technology School of Aerospace Engineering Atlanta, Georgia 30332	ENG/CBT	CBT 8414906
	4. Award Period From 10/1/85 To 3/31/89	5. Cumulative Award Amount $187,209

6. Project Title

Effects of Pressure in Turbulent Reacting Flows

PART II—SUMMARY OF COMPLETED PROJECT *(FOR PUBLIC USE)*

In turbulent reacting flows, analytical description requires knowledge of some covariances of pressure fluctuations with other quantities such as velocity fluctuations and their space derivatives. Both theory and experiment have failed to yield reliable information on such quantities. This program was initiated to provide information on the needed quantities in a simple turbulent premixed flame. Two component laser velocimetry, Rayleigh scattering and dynamic Pitot barometry were used for simultaneous velocity, density and pressure-scalar gradient correlation. It was found that, while the pressure-velocity and pressure-scalar measurements could be reliably made, measurement inaccuracies prevented reliable spatial gradient measurements. Consequently, a new technique was proposed requiring space-separated velocity and velocity-scalar correlations. The end of the program came during development of the space-separated laser beam apparatus.

PART III—TECHNICAL INFORMATION *(FOR PROGRAM MANAGEMENT USES)*

1. ITEM *(Check appropriate blocks)*	NONE	ATTACHED	PREVIOUSLY FURNISHED	TO BE FURNISHED SEPARATELY TO PROGRAM: Check (✓)	Approx. Date
a. Abstracts of Theses	X				
b. Publication Citations		X			
c. Data on Scientific Collaborators		X			
d. Information on Inventions	X				
e. Technical Description of Project and Results		X			
f. Other *(specify)* Paper under review		X			

2. Principal Investigator/Project Director Name *(Typed)*	3. Principal Investigator/Project Director Signature	4. Date
Warren C. Strahle		4/25/89

NSF Form 98A (1-87) Supersedes All Previous Editions

Form Approved OMB No. 3145-005[illegible]

PUBLICATION CITATION

1. Strahle, W.C., "Pressure-Strain and Pressure-Scalar Gradient Correlations in Variable Density Turbulent Flows," AIAA Journal, 26, pp.969-973 (1988).

2. Waldherr, G.A., deGroot, W.A., and Strahle, W.C., "Pressure-Scalar Correlations in a Turbulent Reacting Flow" (submitted to Combustion and Flame), 1988.

SCIENTIFIC COLLABORATORS

1. Dr. Wilhelmus A. DeGroot, Research Engineer.

2. Mr. Gregor A. Waldherr, Graduate Research Assistant.

TECHNICAL DESCRIPTION OF OF PROJECT AND RESULTS

The material which follows is taken from a proposal to the NSF. It accurately reflects the progress on the project.

SCIENTIFIC COLLABORATORS

1. Dr. Wilhelmus A. DeGroot, Research Engineer.

2. Mr. Gregor A. Waldherr, Graduate Research Assistant.

NATIONAL SCIENCE FOUNDATION

PROJECT SUMMARY

FOR NSF USE ONLY			
DIRECTORATE/DIVISION	PROGRAM OR SECTION	PROPOSAL NO.	F.Y.

NAME OF INSTITUTION (INCLUDE BRANCH/CAMPUS AND SCHOOL OR DIVISION)

Georgia Institute of Technology
School of Aerospace Engineering

ADDRESS (INCLUDE DEPARTMENT)

Atlanta, GA 30332

PRINCIPAL INVESTIGATOR(S)

Warren C. Strahle

TITLE OF PROJECT

Indirect Nonintrusive Determination of Pressure Correlations in Turbulent Reacting Flows

TECHNICAL ABSTRACT (LIMIT TO 22 PICA OR 18 ELITE TYPEWRITTEN LINES)

Past Experience in intrusive measurement in flames has yielded serious error in determination of pressure containing correlations in a turbulent reacting flow. A new technique which indirectly determines these correlations is proposed, which, at the same time, is totally nonintrusive. At issue are the pressure-velocity, pressure-strain, pressure-scalar and pressure-scalar gradient correlations. Comparison of the results with past intrusive measurements will be made and comparison with theory will be carried out. Theory will be modified as necessary. The technique proposed uses an exact solution for the pressure in terms of density and velocity fluctuations, which are to be measured nonintrusively by two point space separated laser methods.

NSF Form 4 (7-83)

RESULTS FROM PRIOR NSF SUPPORT

Prior Award: Grant No. CBT-8414906 $187,209
10-1-85 to 9-30-88

Title: Effects of Pressure in Turbulent Reacting Flows

Summary:

Laser velocimetry, Rayleigh molecular scattering and intrusive dynamic Pitot barometry have been used in a premixed turbulent flame in an attempt to measure pressure-containing turbulence correlations. A new theory for the pressure-strain and pressure-scalar gradient correlations was developed. Many of the results of the program are contained in the following section of this proposal. However, there has been a dominant difficulty which has been encountered, especially with correlations involving a spatial derivative such as the strain rate or scalar gradient. Using the dynamic Pitot barometer the results depend upon subtraction of several large numbers containing experimental error to obtain a much smaller number. Adding to this the fact that there are some intrusiveness issues with the barometer, the dominant scientific conclusion of the program will most probably be that the pressure-containing correlations should not be attacked in this manner. A new method of attack has been discovered, however, and forms the basis for this proposal. Because this method requires a strong change of technique this proposal is to be considered new, rather than a request for renewal.

Publications:

1. Strahle, W. C., "Pressure-Strain and Pressure-Scalar Gradient Correlations in Variable Density Turbulent Flows," AIAA Paper No. 87-1351 (accepted for publication in AIAA Journal, 1988)

2. Waldherr, G. A., de Groot, W. A. and Strahle, W. C., "Pressure-Scalar Correlations in a Turbulent Reacting Flow," submitted to Combustion and Flame.

PROJECT DESCRIPTION

Introduction

The state variable pressure and its gradient in both average and fluctuation form enter into turbulence descriptions in troublesome ways. Problems arise with the pressure in constant density flows, and these problems are compounded in variable density situations such as in turbulent reacting flows. In time averaged treatment of the field equations the difficulty begins at the level of closure of the turbulent kinetic energy equation and becomes more severe if one proceeds to conservation of turbulent stresses and scalar transport.(1) The problems are also inescapable in probability density function evolution descriptions of turbulence.(2)

The quantities of interest in this proposal, as they occur in their most primitive form in stress transport and scalar transport equations, are

$$C_{k\ell} \equiv \overline{v_k'' \, \partial p/\partial x_\ell} \qquad (1)$$

$$D_\ell \equiv \overline{c'' \, \partial p/\partial} x_\ell \qquad (2)$$

The quantity $C_{k\ell}$ is a second order tensor where v_k is the velocity in the k^{th} direction, p is pressure, and x_ℓ is the ℓ^{th} Cartesian coordinate direction. The vector D_ℓ contains the scalar, c, which may be density, mass fraction, enthalpy etc. Here the overbar denotes a time average, and the double prime denotes a Favre fluctuation where, for example,

$$v_k = \tilde{v}_k + v_k''$$

and $\tilde{v}_k$ is the Favre average (mass weighted average). Regular time averages will be denoted by a single prime superscript, as, for example with

$$p = \overline{p} + p'$$

In constant density flows Favre and conventional averages are identical.

Because there are some advantages in physical interpretation, at least for constant density flows, and some advantages in measurement, Eqs. (1) and (2) are usually expanded as

$$C_{k\ell} = \underbrace{\overline{v''_k} \frac{\partial \bar{p}}{\partial x_\ell}}_{I} + \underbrace{\frac{\partial}{\partial x_\ell} (\overline{p' \, v''_k})}_{II} - \underbrace{\overline{p' \frac{\partial v''_k}{\partial x_\ell}}}_{III} \tag{3}$$

$$D_\ell = \underbrace{\overline{c''} \frac{\partial \bar{p}}{\partial x_\ell}}_{IV} + \underbrace{\frac{\partial}{\partial x_\ell} (\overline{c'' p'})}_{V} - \underbrace{\overline{p' \frac{\partial c''}{\partial x_\ell}}}_{VI} \tag{4}$$

The contracted form of Eq. (3), which appears in the turbulent kinetic energy equation, is

$$C_{\ell\ell} = \underbrace{\overline{v''_\ell} \frac{\partial \bar{p}}{\partial x_\ell}}_{VII} + \underbrace{\frac{\partial}{\partial x_\ell} (\overline{p' v''_\ell})}_{VIII} - \underbrace{\overline{p' \frac{\partial v''_\ell}{\partial x_\ell}}}_{IX} \tag{5}$$

The following points concerning Eqs. (3)-(5) are now noted:

1. In constant density and scalar flows terms I, IV and VII disappear since

$$\overline{v''_k} = \overline{c''} = \overline{v'_k} = \overline{c'} = 0$$

2. Term III, called the pressure-strain term, is regarded as "redistributive" in constant density turbulence since, upon contraction, term IX is zero in such flows and this term does not contribute to the turbulent kinetic energy. Term III loses this distinction in variable density flows.
3. Terms II, V and VIII look diffusive in nature and are usually so treated; however, this treatment is challenged below.

4. Terms II, V and VIII do not actually require the distinction between Favre and conventional fluctuations since, for example,

$$\overline{p'v_k''} = \overline{p'(v_k - \tilde{v}_k)} = \overline{p' \ (\bar{v}_k + v_k' - \tilde{v}_k)} = \overline{p'v_k'} \qquad (6)$$

Term III has been elaborately modelled by Launder et al[3] for constant density flows with use of prior work of Rotta.[4] Together with a modification by Lumley[5], Jones[1] suggests direct use of the constant density pressure-strain correlation in variable density flows, as long as conventional averages are replaced by Favre averages. Following Lumley's approach[6], term VI has been suggested by Jones[1] to be modelled in a fashion close to that of term III.

Admitting that justification was lacking, Bray et al[7] simply neglect all terms containing the pressure fluctuations (II, III, V, VI, VIII, IX). Kollmann and Vandrome[8] neglect only IX in Eq. (5), arguing that dilation fluctuations are much smaller than vortical fluctuations. Bilger[9] and Starner and Bilger[10] also argue that IX should be neglected on the grounds that an undirected volume expansion interacting with a pressure fluctuation appears acoustic in nature and should probably not contribute to the turbulence energy. Borghi and Escudie[11] retain terms VI and IX in their work although the grounds for the models used are not clear. Virtually all workers retain terms I, IV and VII when they appear and the physical effects of these terms are usually quite striking.

Except where neglected, terms II, V and VIII are always treated as diffusive and are lumped into another diffusive term appearing in the transport equation. The problem is that pressure is not diffusive. In constant density flows it is well known that the initial value problem in vortex dynamics can be solved without consideration of pressure. Pressure is then determined by solution of a Poisson equation which determines pressure at a point in terms of the entire acceleration field. In compressible flows an acoustic equation determines p' which has the same property; the pressure at a point is determined by events occurring over the entire field and not by the local carriage of fluid lumps. Moreover, in linear acoustics the quantity $\overline{p'v_k'}$ is the acoustic intensity, if the Mach number is low, and this quantity is certainly not diffusive in nature.

More damning evidence against treatment of the middle terms of Eqs. (3)-(5) as diffusion terms comes from experiment. Indirect measurements of VIII by Townsend(12) and direct measurement by Kobashi(13) show an unfavorable comparison of VIII with the diffusion of kinetic energy. Shown in Fig. 1 are Townsend's cylinder wake results. The results are even worse in the case of Laufer's(14) pipe flow data where the pressure "diffusion" term is of opposite sign to the turbulence kinetic energy diffusion. Shown in Fig. 2 are results obtained at this laboratory (to be discussed later) comparing the $\overline{p'v'}$ term to the radial normal stress gradient moving radially outward in a premixed axially symmetric propane-air flame. Again, there is no correspondence between the two, suggesting that, even if gradient diffusion of kinetic energy were a proper description, the pressure-velocity term does not belong in this category.

The often neglect of terms III, VI and IX is also probably not correct. For example, concerning term IX, in the vorticity transport equation there is a strong effect of dilation-vorticity interaction. Consequently, in strongly dilating flows term IX can be expected to affect the turbulence energy.

The pressure-strain term (terms III and IX) have been recently measured indirectly(15) in a hydrogen-air diffusion flame and shown to be important in

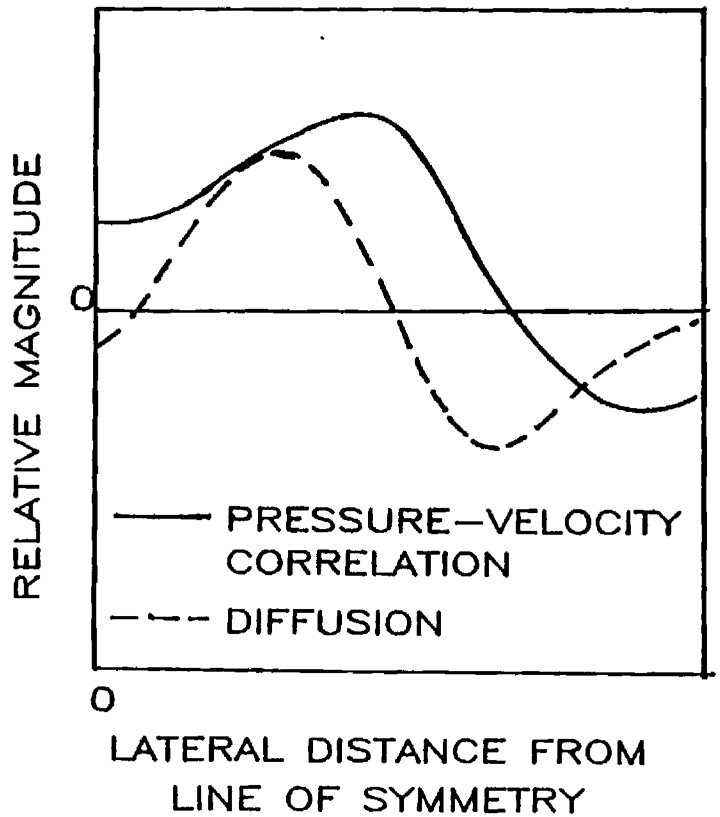

Figure 1. Townsend's circular cylinder wake results. Comparison of pressure-velocity term with diffusion of turbulent kinetic energy.

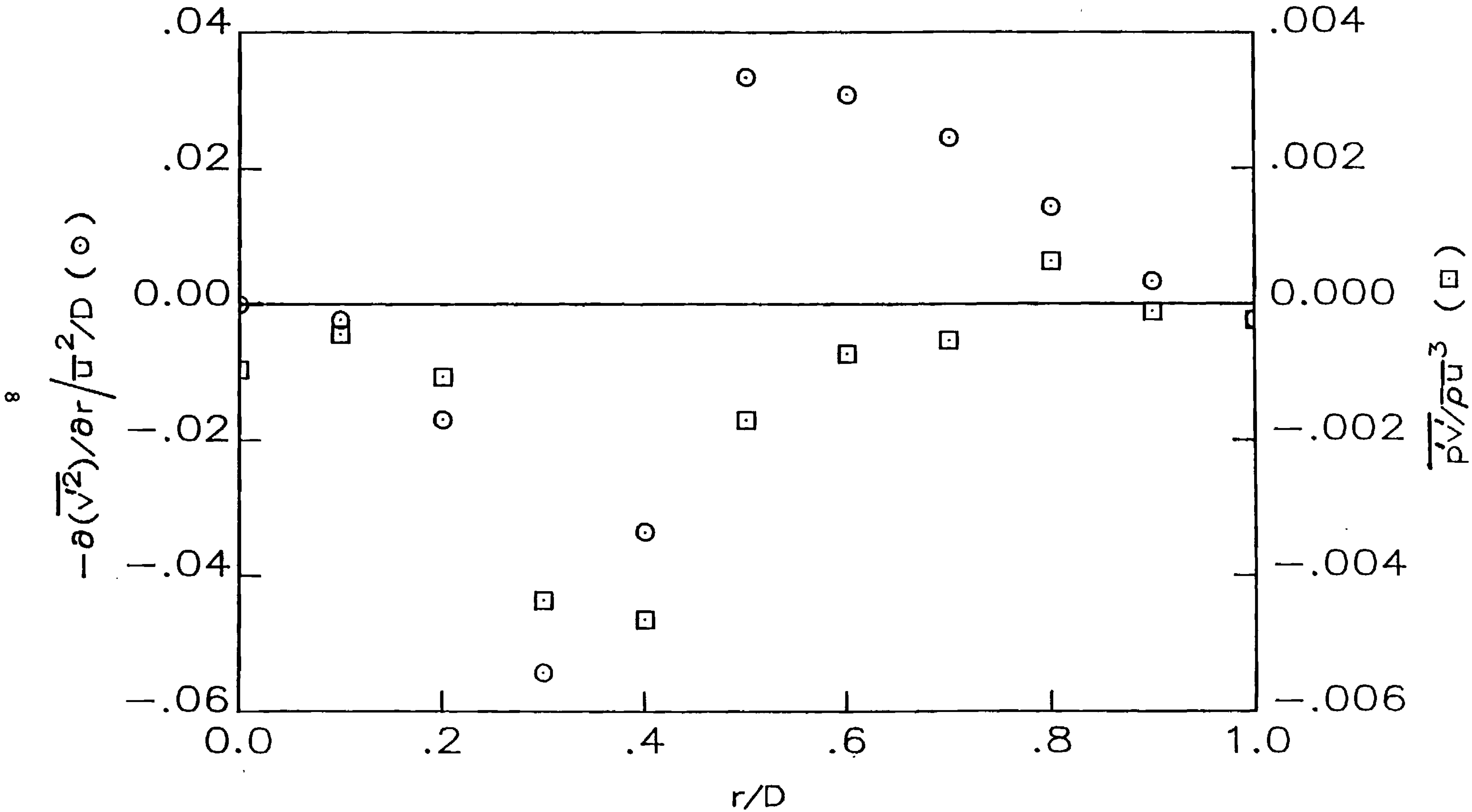

Figure 2. Comparison of $\overline{p'v'}$ with diffusion of the radial normal stress in a premixed flame.

stress transport. A new model for these terms has been developed[16] under a current program, but experimental verification is required.

The conclusion is that the situation is poor with regard to knowledge of $C_{k\ell}$ or D_{ℓ}, especially in turbulent reacting flows. There are also severe problems in the constant density limit. New models need to be developed in concert with experimentation for verification and model suggestions. This proposal addresses this need.

<u>Background at this Laboratory</u>

Two prior programs have been run at his laboratory attacking terms II, III, V and VI of Eqs. (3) and (4) from both theoretical and experimental points of view. Measurements have been made on fuel lean propane-air flames and stoichiometric methane-air flames, both of which were premixed. The flame geometry is shown in Fig. 3. It is seen that the shear layer between the jet flow and surroundings does not penetrate to the flame zone, so that the flame process is basically adiabatic.

Results on this and a companion flame are located in Refs. (17)-(19). Shown in Figs. 4 and 5 are the axial and radial traverses of the cross correlation, and its coefficient, of p' and the axial velocity fluctuation. A typical curve of the same quantities, but with the radial velocity, is shown in Fig. 6. At first sight, there appears only weak correlation in the active reaction region and high correlation outside. However, when the divergence of $\overline{p'v_i'}$ is constructed from these data (to obtain Term VIII of Eq. (5)), it is found that it is as large as any other term in the turbulent kinetic energy equation and therefore plays a role in energy transport throughout the flame; $\overline{p'v'}$ effects cannot be neglected. Moreover, it is dominantly a source of kinetic energy, although at certain locations it is a weak sink.

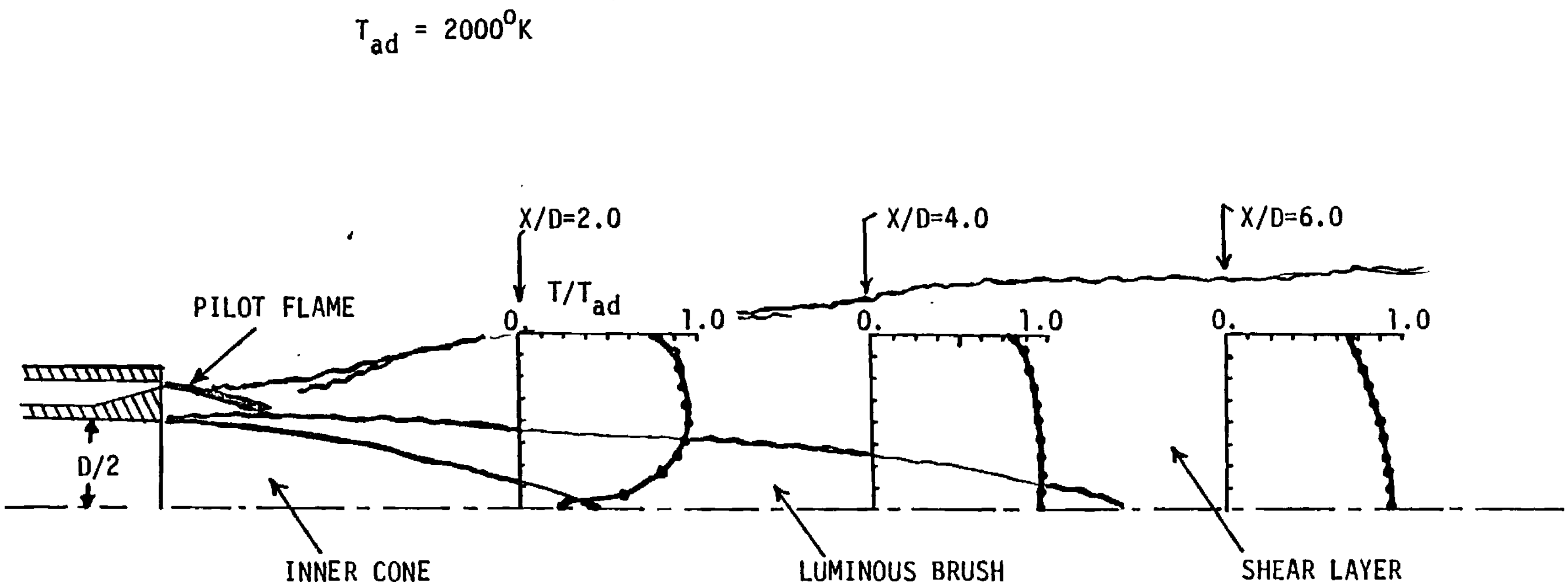

Figure 3. Premixed flame geometry and temperature profiles.

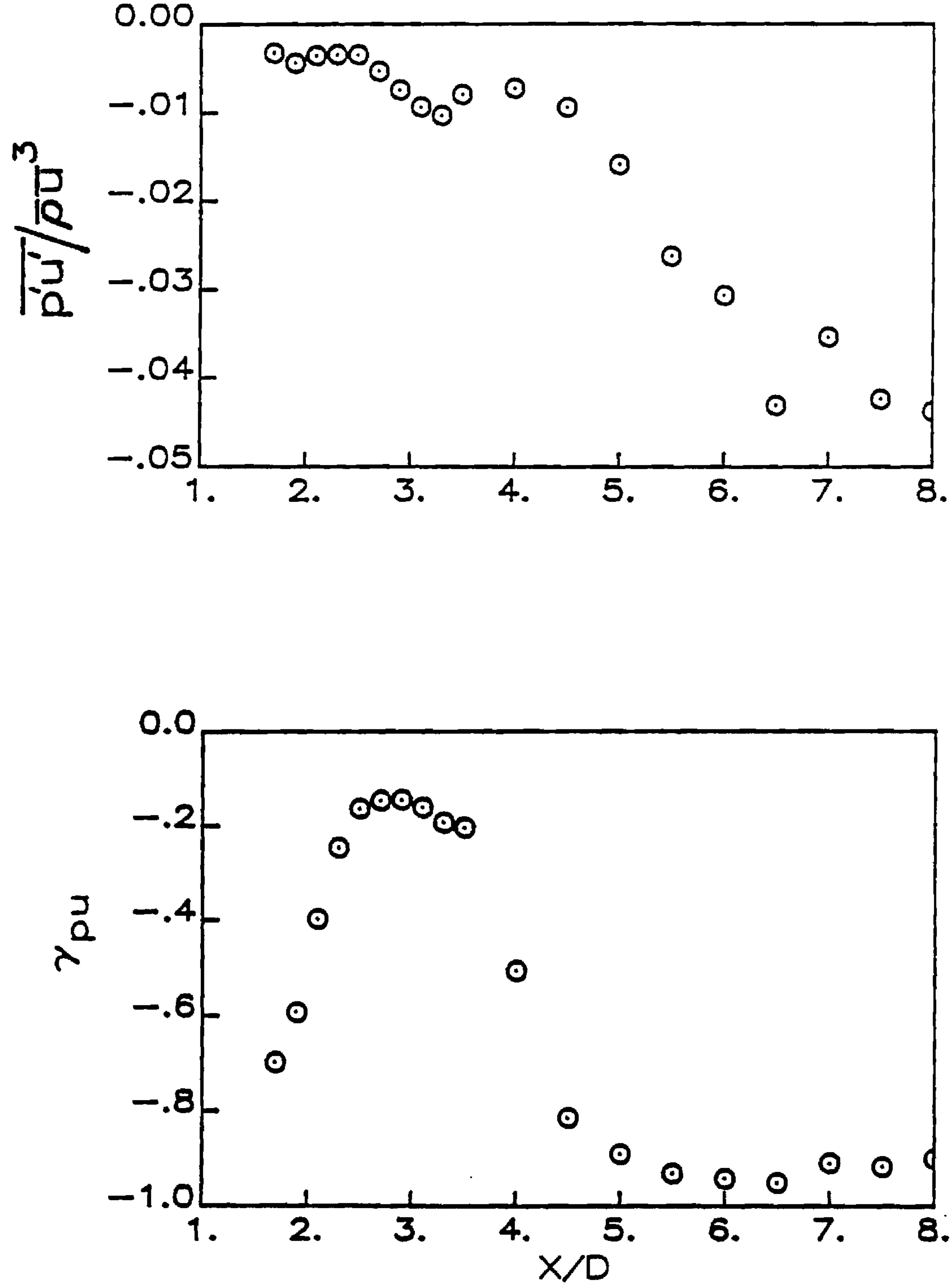

Figure 4. Correlation of $\overline{p'u'}$ and its coefficient along the axis of the premixed flame.

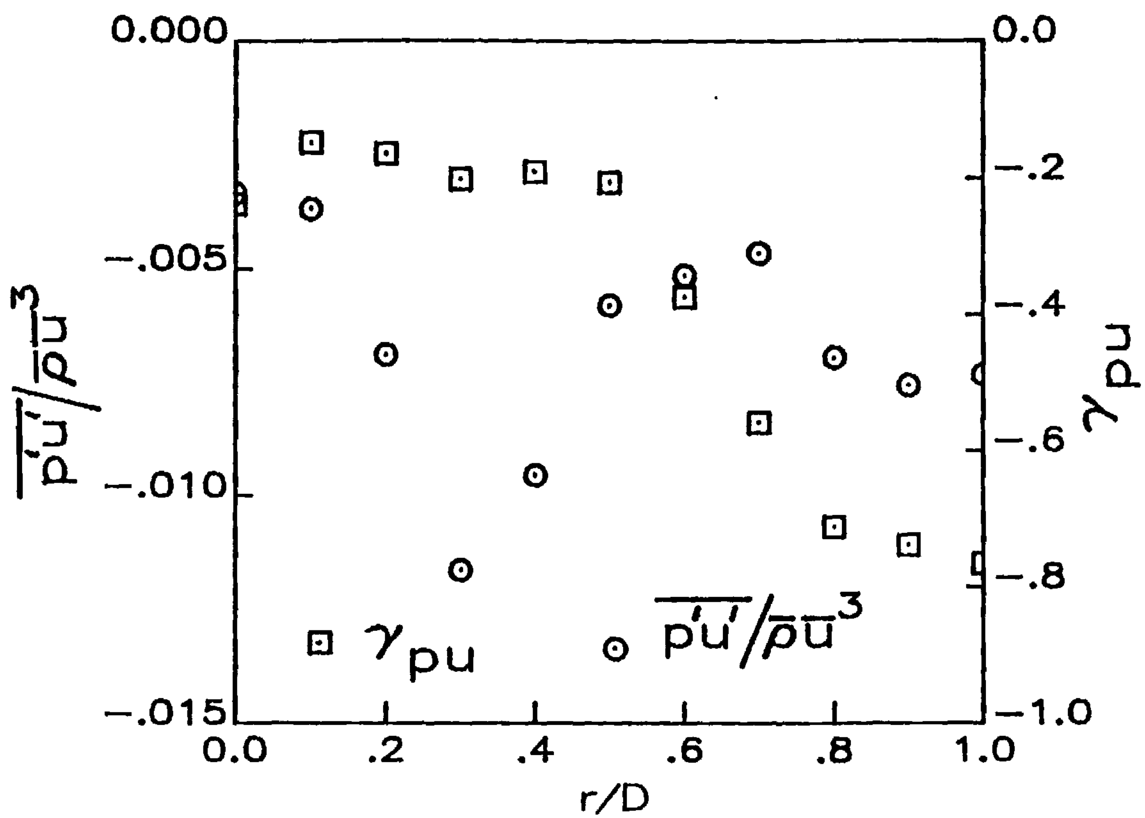

Figure 5. Correlation of $\overline{p'u'}$ and its coefficient along a radius.

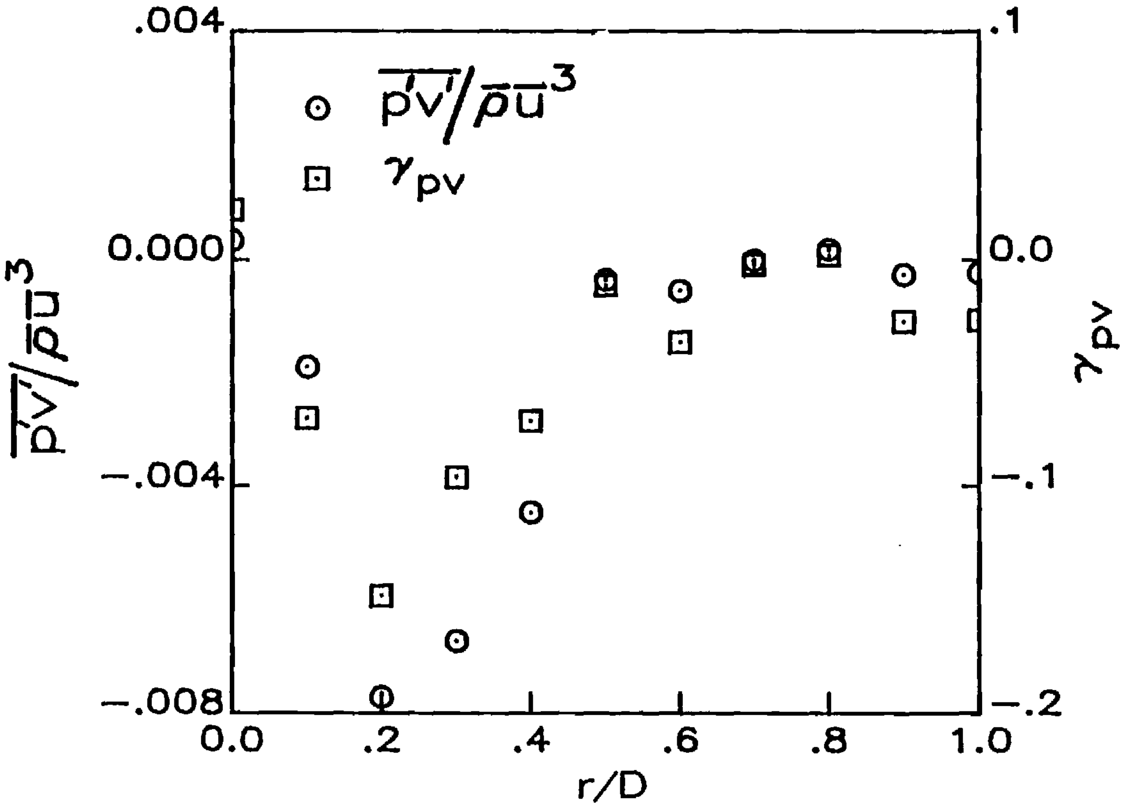

Figure 6. Correlation of $\overline{p'v'}$ and its coefficient along a radius.

A surprising aspect of these measurements is the extremely high (negative) cross correlation coefficient of the pressure and axial velocity fluctuation in regions outside the reaction region. What is found in these regions is that, approximately, $p' = -\bar{\rho}\,\bar{u}\,u'$, implying the total head is not fluctuating. Some theoretical support for this may be found in Ref. 20. However, the result does not yield Galilean invariance to $\overline{p'u'}$, as it must have. Consequently, $\bar{u}$ must be interpreted as some relevant velocity difference of the order of the mean flow velocity, rather than the mean velocity itself.

The above results have been obtained by a combination of intrusive and non-intrusive probes. Intrusive means have been heat flux probes, thermocouple thermometry and Pitot barometry. Non-intrusive methods have been laser velocimetry and molecular Rayleigh scattering thermometry. The crucial measurement, in the present context, is the measurement of pressure. Nonintrusive techniques[21] do not have the sensitivity, as yet, to measure pressure fluctuations of the order of 0.01% of the mean pressure, which occurs in these flows. Nonintrusive sensing of temperature and density, which is possible, will, in principle, yield pressure through the equation of state. However density and temperature fluctuations in flames are of the order of the mean quantities themselves while the pressure fluctuation is small; consequently this method will fail because of experimental inaccuracies. Therefore, intrusive probes have been used. Usual static pressure probes are undesirable because of angle of attack fluctuations and thermal disturbances of the usual leading surface on such probes. Consequently, a microphone Pitot probe, shown in Fig. 7, was used.

The Pitot tube measures the total pressure well[22] at angles of attack up to 10° and if the stagnation time is short compared with the reciprocal of an upper frequency limit of interest. Moreover, there is no thermal

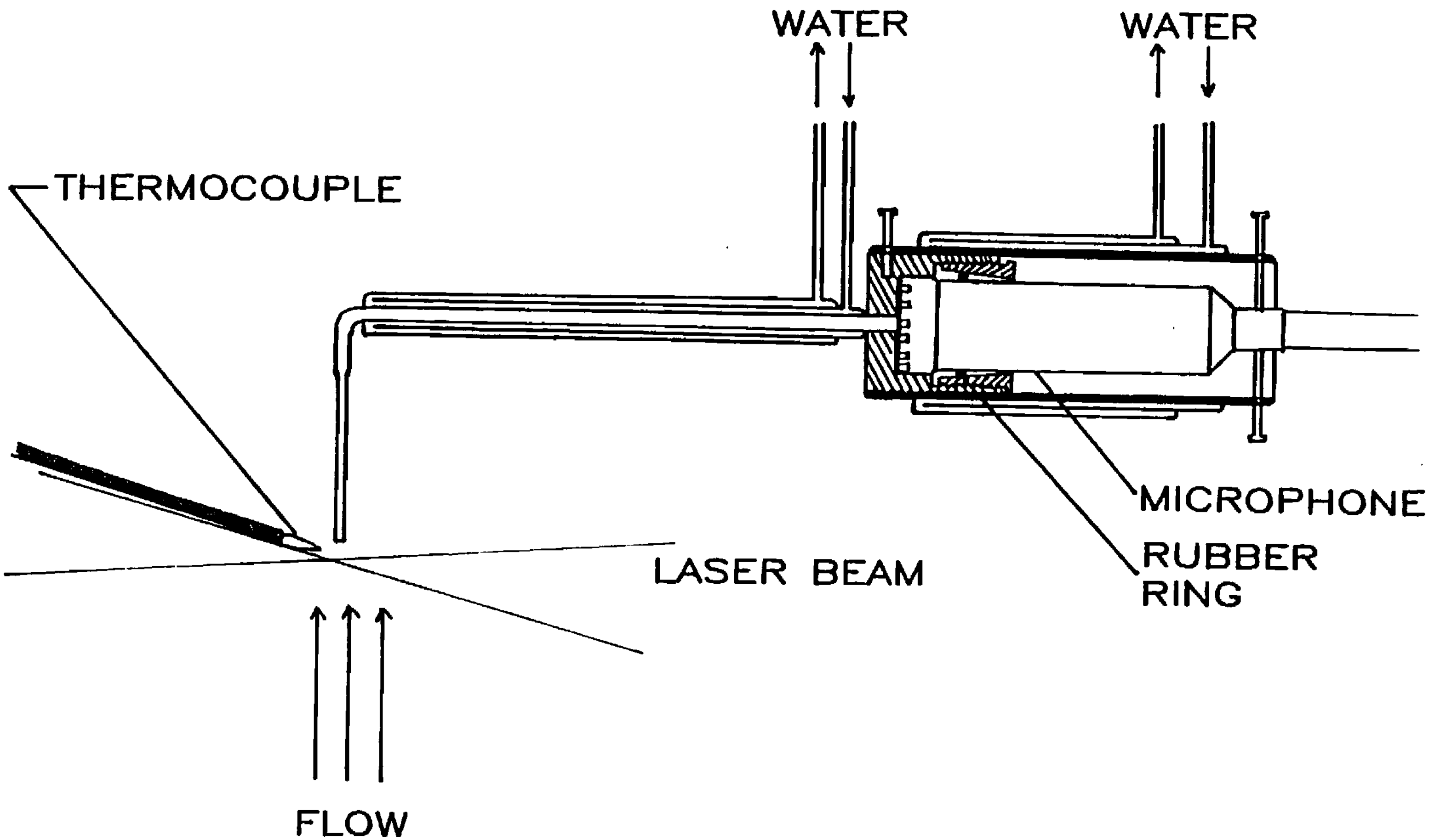

Figure 7. Instrumentation configuration for latest work.

disturbance to the stagnating streamline if the Reynolds number is high. All necessary restrictions were met with the flows investigated and for the probe size involved, so the total pressure fluctuation at the probe tip is

$$P_T' = p' + \frac{1}{2}(\rho u^2)' \tag{7}$$

There are four problems. First, the long tube to the microphone introduces a sensing path that makes the microphone reading not equal to P_T'; that is, frequency compensation is required. Secondly, when expanded, Eq. (7) is nonlinear in the fluctuating quantities. Thirdly, in order to extract the static pressure, simultaneous measurement is required of velocity and density. Finally, there is the issue of what density to sense, since in a premixed flow the probe may act as a flameholder.

Fortunately, by direct measurement it was determined that the only terms important in the expansion of Eq. (7) are

$$P_T' \quad p' + \overline{\rho}\overline{u}u' + \frac{1}{2}\rho'\overline{u}^2 \tag{8}$$

and Eq. (8) becomes the working equation after frequency compensation. Frequency calibration must be accomplished for several probe tip temperatures because the frequency response depends upon the gas column temperature in the probe. A transfer function is generated so that the Fourier transforms are related by

$$P_{T_{true}} = H_{\omega_{P_T}} P_{T_{sensed}} \tag{9}$$

where capital letters denote transforms and H_ω is the temperature dependent transfer function. One has the option of working in the frequency domain with Eq. (9) or in the time domain

$$P_{T_{true}}' = \int_0^\infty h_{P_T}(t)\, P_{T_{sensed}}'(t - \tau)\, d\tau \tag{10}$$

where h(t) is the inverse transform of $H_{\omega_{P_T}}$,

Concerning the flameholding problem, none was visibly observed, but even if it had it would introduce little error. This results from the fact that the change in dynamic pressure in going across a flame is of the order of ρS_L^2, where S_L is the laminar flame speed of the mixture. In our case this is small compared with the dynamic heads measured.

One other restriction in the practical use of Eq. (7) is that the static pressure fluctuation should be of the same order as the total pressure fluctuation so that upon subtraction of the dynamic head from the total pressure there are still significant digits left. As mentioned this restriction was met in prior programs for pressure velocity correlations. However, a severe problem has arisen in pressure-scalar correlations and this problem will form the basis for this proposal.

Velocity measurement has been carried out by a two component, 5 w Argon-ion laser velocimeter, using counter processing. Simultaneous Rayleigh scattering measurements have been most recently used for density measurement (the most easily obtained scalar). After and before LV particle arrival, 20 points of the Rayleigh signal, sampled at 8 usec intervals, are used for density determination. Using a new technique for[23] background noise extraction from the Rayleigh signal both density and velocity and their correlation may be obtained.

The fundamental problem which has been uncovered is that the pressure-scalar and the pressure-scalar gradient correlations are subject to high error because a) the correlations of the Pitot barometer and density are large, b) the correlation of the Pitot barometer and velocity are large, but c) the true correlation of interest requires subtraction of these numbers to yield a small quantity as is illustrated in Figs. 8 - 10. The raw

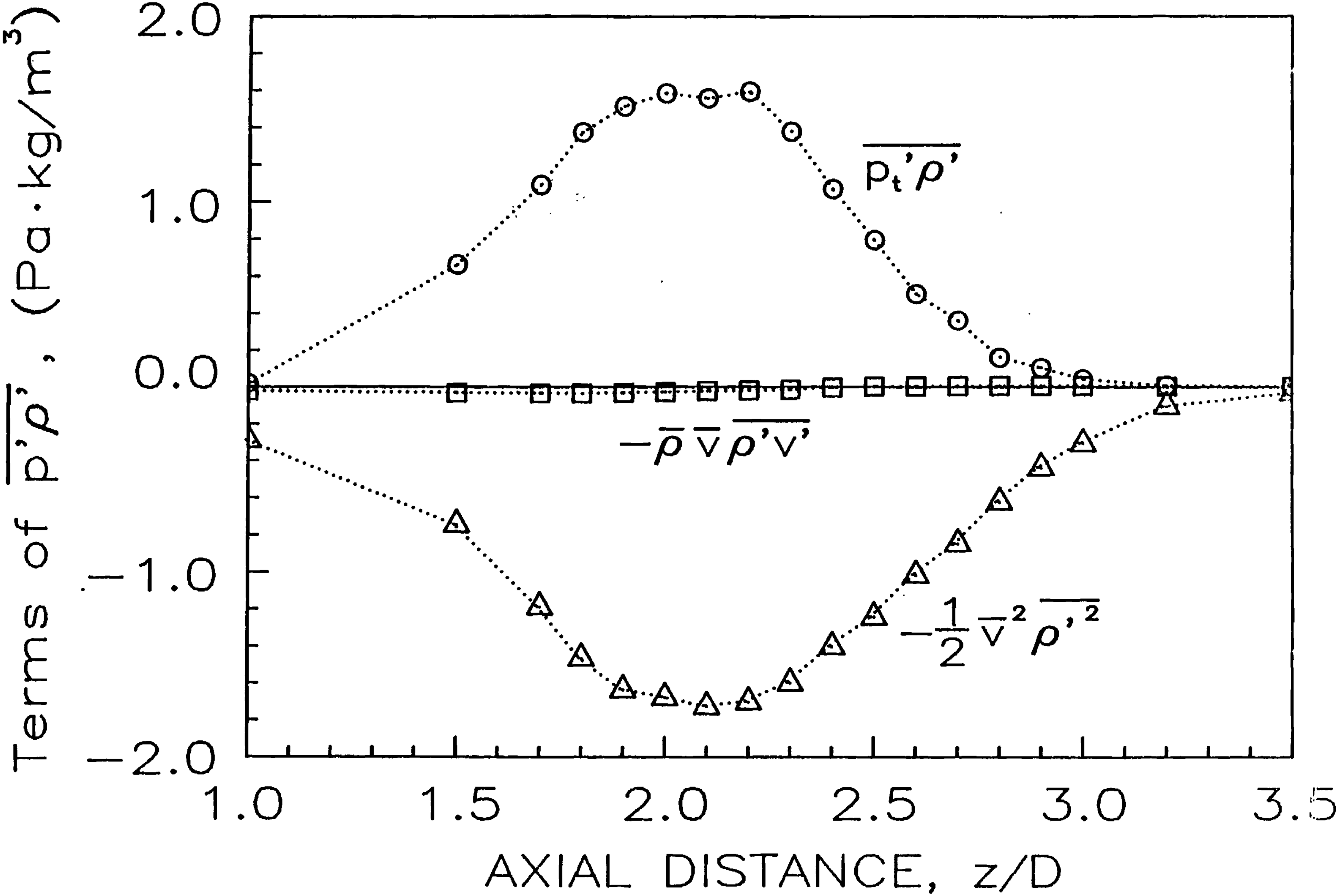

Figure 8. Correlations required for determination of the pressure-scalar correlation.

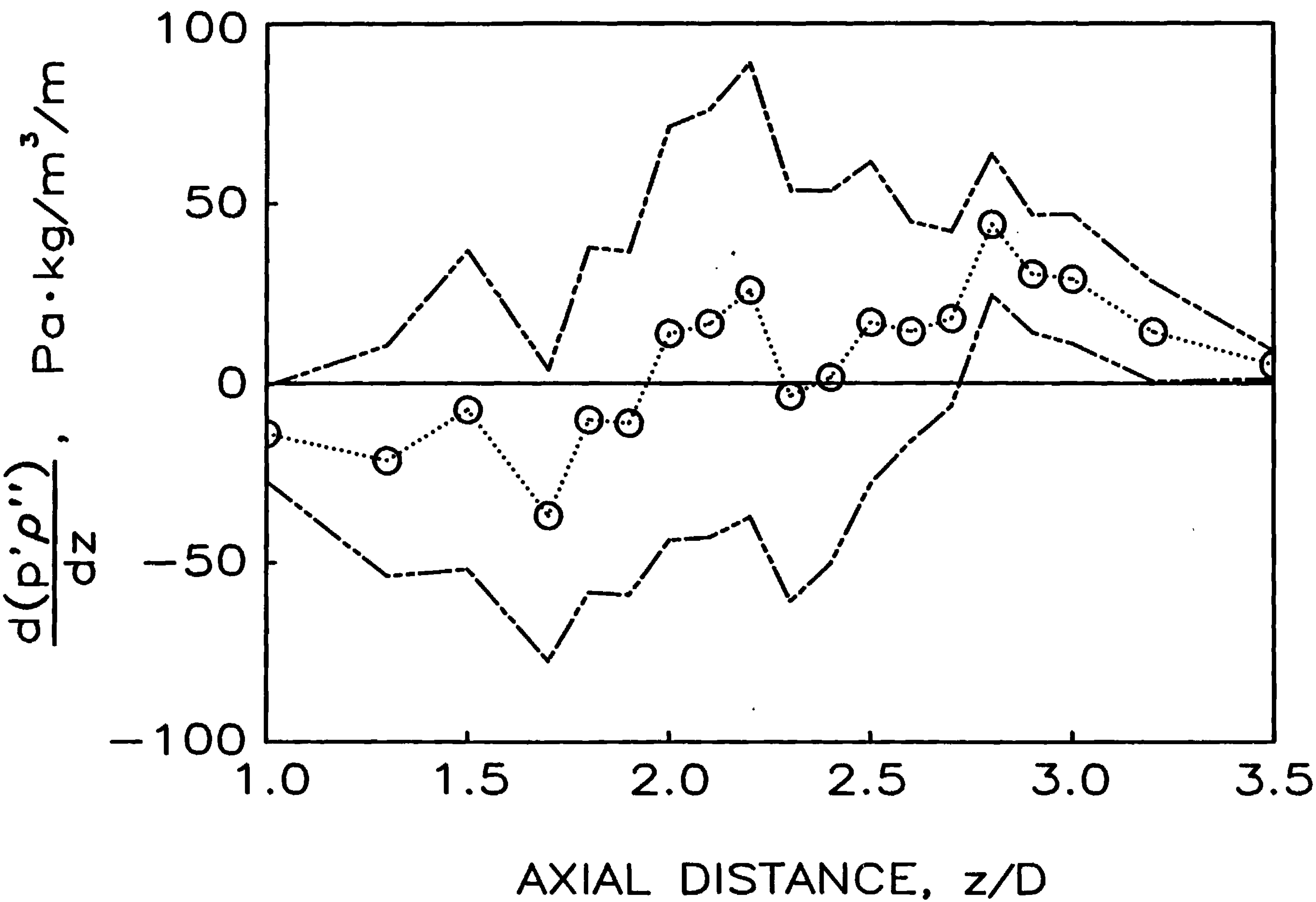

Figure 9. Axial derivative of pressure-scalar correlation on the flame axis.

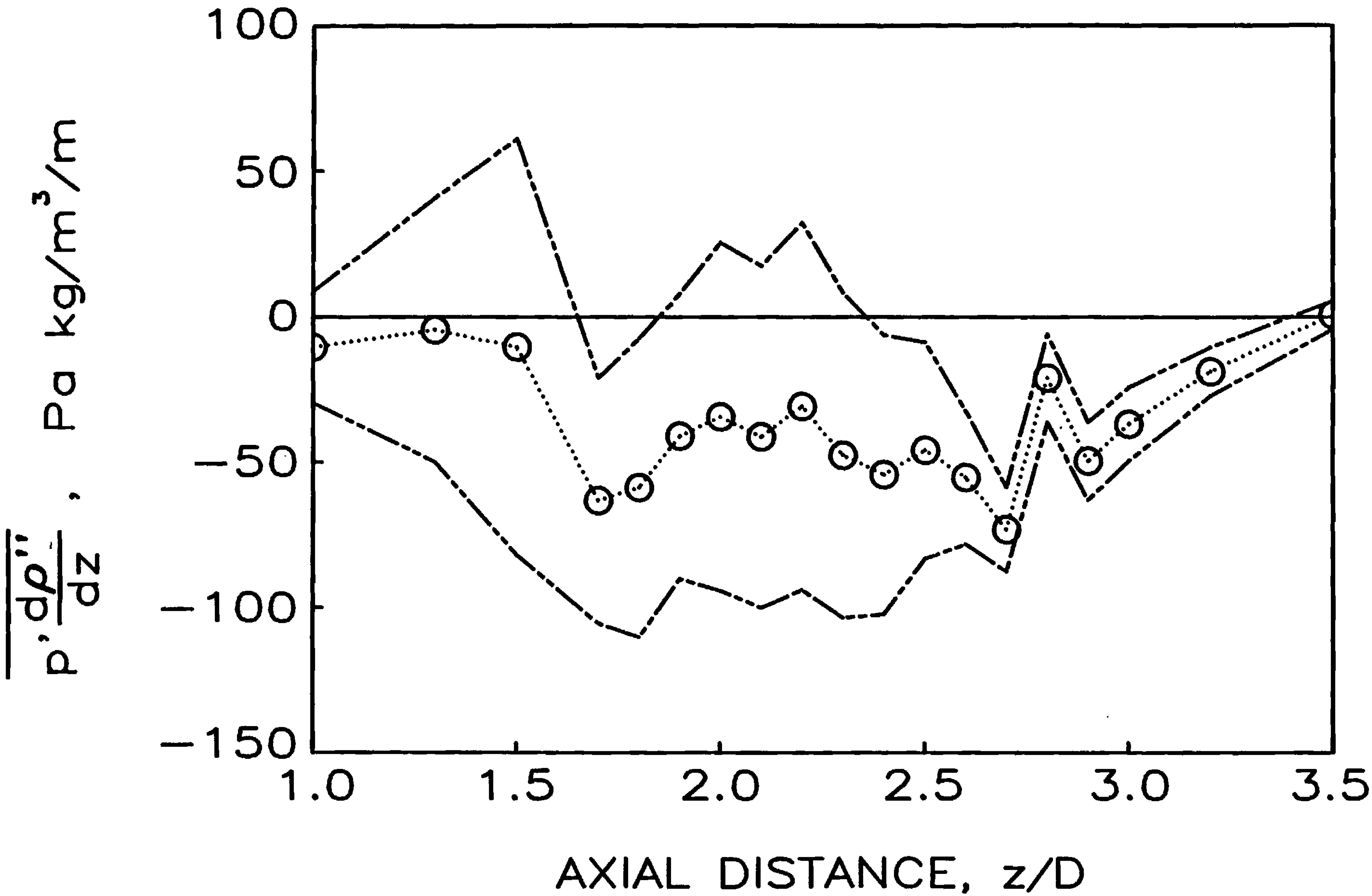

Figure 10. Pressure-scalar gradient correlation on the flame axis.

measurements are shown in Fig. 8 and the derived pressure-density and pressure-density gradient correlations in Figs. 9 and 10. Error bars are shown and they are large. In fact, one can say over most of the range of measurement that no numerical value or sign of the results may be confidently predicted.

A further difficulty is that even if the measurements are taken at face value they appear too large in magnitude. This follows from consideration of the density-velocity covariance transport equation from Ref. (1)

$$\frac{\partial}{\partial x_j}\left(\overline{\rho' v_i''} \ \tilde{v}_j \right) = -\left(\overline{\rho' v_j''}\frac{\partial \tilde{v}_i}{\partial x_j} + \overline{v_i'' \ v_j''}\frac{\partial \bar{\rho}}{\partial x_j} \right)$$

$$- \frac{1}{\bar{\rho}}\left[\frac{\partial}{\partial x_i}\overline{\rho' p'} - \overline{p' \frac{\partial \rho'}{\partial x_i}} \right] \tag{11}$$

$$- \bar{\rho}\frac{\partial}{\partial x_j}\left(\frac{\overline{\rho' v_i'' \ v_j''}}{\bar{\rho}} \right) - \bar{\rho}\ \overline{v_i'' \frac{\partial v_j''}{\partial x_j}}$$

The bracketed term on the right side of Eq. (11) is of issue as a source for the $\overline{\rho' v_i''}$ correlation. If the magnitudes implied by Figs. 9 and 10 were correct, a value of $\overline{\rho' v_i''}$ at least a factor of 5 too high would result as compared with actual measurement, shown on the flame axis in Fig. 11.

As the current program continues efforts will be made to reduce the errors and make as much progress as possible with the current set-up. However, it is desired to a) get rid of the intrusive Pitot tube for several reasons, b) do completely non-intrusive measurements and c) be guaranteed that the magnitude of the result is correct. Fortunately we think there is a way to do this and this proposal is for a program to do just this. What has been accomplished in the past was a direct but intrusive measurement; what is proposed is an indirect, nonintrusive set of measurements.

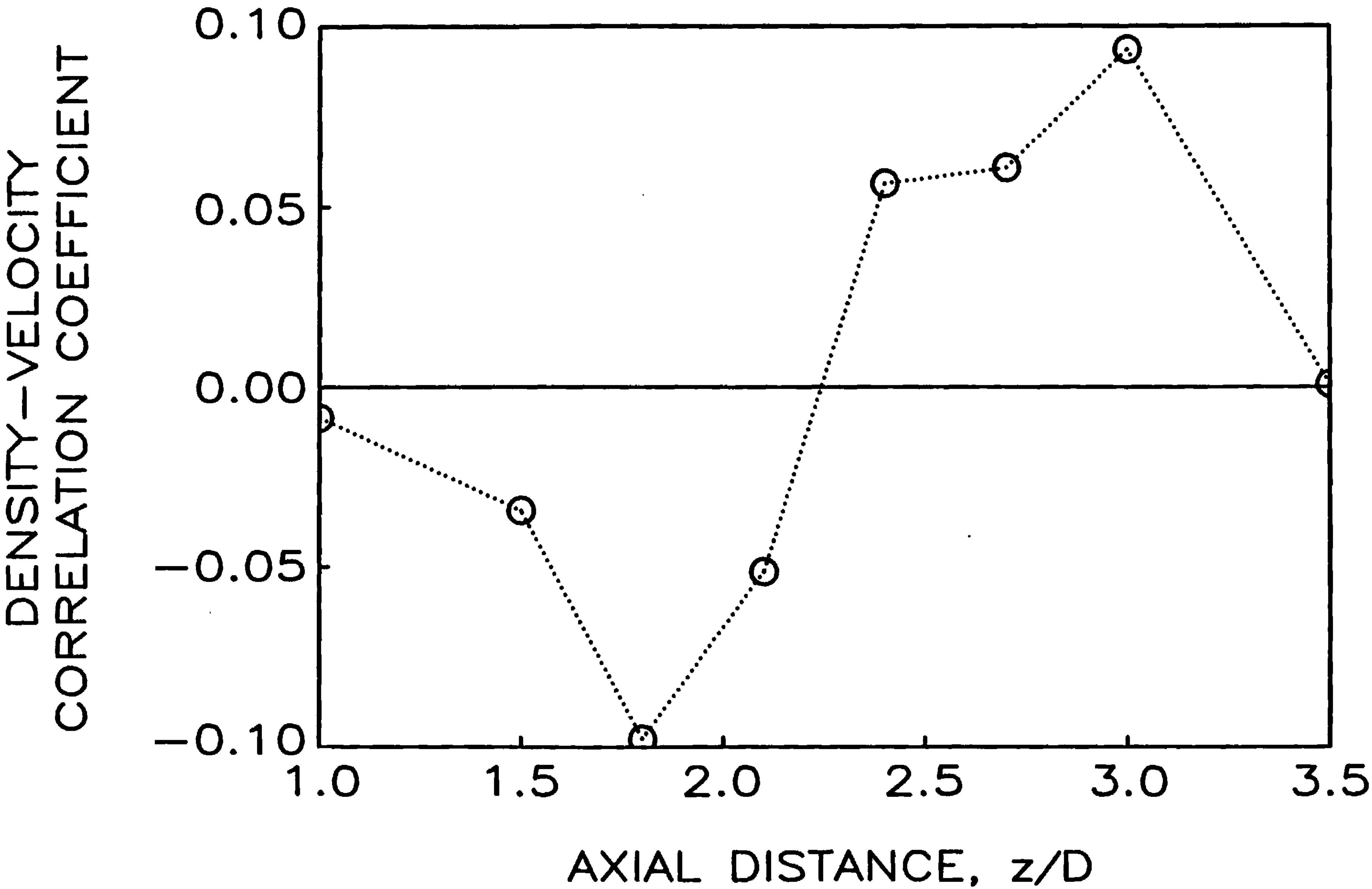

Figure 11. Density - velocity correlation coefficient on the flame axis.

Proposed Program:

For general variable density flows which are not wall bounded, the pressure fluctuation is given by[16]

$$P' (x_i, t) = \int dV (y_i) \; G (x_i, y_i) \; F (y_i) \tag{12}$$

with

$$F = - \frac{\partial^2 \rho}{\partial t^2} + 2 \frac{\partial^2}{\partial x_i \partial x_j} \left(\rho' \tilde{v}_j v_i'' \right) + \frac{\partial^2}{\partial x_i \partial x_j} \left(\rho v_i'' v_j'' - \overline{\rho v_i'' v_j''} \right)$$
$$+ 2 \frac{\partial^2}{\partial x_i \partial x_j} \left(\bar{\rho} \tilde{v}_j v_i'' \right) \tag{13}$$

and G the free space Greens function

$$G = \frac{1}{4\pi r} \qquad r = \sqrt{(y_i - x_i)(y_i - x_i)}$$

The only approximation made in Eqs. (12) and (13) is that molecular viscosity effects are excluded, and this is an excellent approximation for the frequencies of the energy containing eddies which contribute most to correlations constructed with Eq. (12). One now multiplies Eq. (12) by either velocity or density fluctuations or rate of strain or scalar gradient and time averages. The result is that in principle only scalar and velocity correlations, albeit space separated at many points, need be measured. These may be measured nonintrusively and pressure may be bypassed.

The initial demonstration of technique, to be compared against prior intrusive measurements, will be made on the correlation of p' and v' along the axis of a methane air premixed stoichiometric flame. It is anticipated that the fourth term on the right side of Eq. (13) will yield the dominant component of the $\overline{p'v_1'}$ correlation (although this will be checked), and this is denoted $\overline{p'v_1'})_4$. As an example of data reduction

$$\overline{p'v_1'})_4 = 2 \int dV(y_i)\, G \frac{\partial^2}{\partial y_i \partial y_j}\left(\bar{\rho}\tilde{v}_j\, \overline{v_i''\,(y_i)\, v_1'\,(x_i)}\right) \tag{14}$$

requires measurement (in addition to mean quantities) of

$$\overline{v_i''\,(y_i)\, v_1'\,(x_i)}$$

for various sets of y_i and x_i. For this and for density measurement the space-separated LV beams of Fig. 12 will be used. The procedure is not without risk, however, for note that space derivatives occur in the integrand of Eq. (14). These derivatives occur on an experimental quantity and would be full of experimental error. The proposed solution around this problem is to transfer the derivatives to the Greens function.

Surrounding the point $x_i - y_i$ with a sphere of size ε and excluding this sphere from the integration of Eq. (12) only introduces an error of order ε compared with unity in a numerical evaluation of Eq. (12), given the experimental data for the integrand. Moreover, again excluding this region, Greens identity may be written as (twice applying the divergence theorem)

$$\int dV\, G \frac{\partial^2}{\partial y_i \partial y_j}\left(\bar{\rho}\tilde{v}_j\, \overline{v_i''\, v_1'}\right) = \int dV\, \bar{\rho}\tilde{v}_j\, \overline{v_i''\, v_1'}\, \frac{\partial^2 G}{\partial y_i \partial y_j} \tag{15}$$

Now the derivatives appear on an analytical function and not the experimental data. The caution is that the second derivative of G tends toward singular behavior as $\varepsilon \to o$ so the results may be numerically sensitive near the region of exclusion. Nevertheless, the advantages of proceeding by this method appear to substantially outweigh the alternative of differentiating the data.

The proposed program would proceed in the following manner:

1. Develop the numerical algorithm to carry out the volume integrations of Eq. (12)

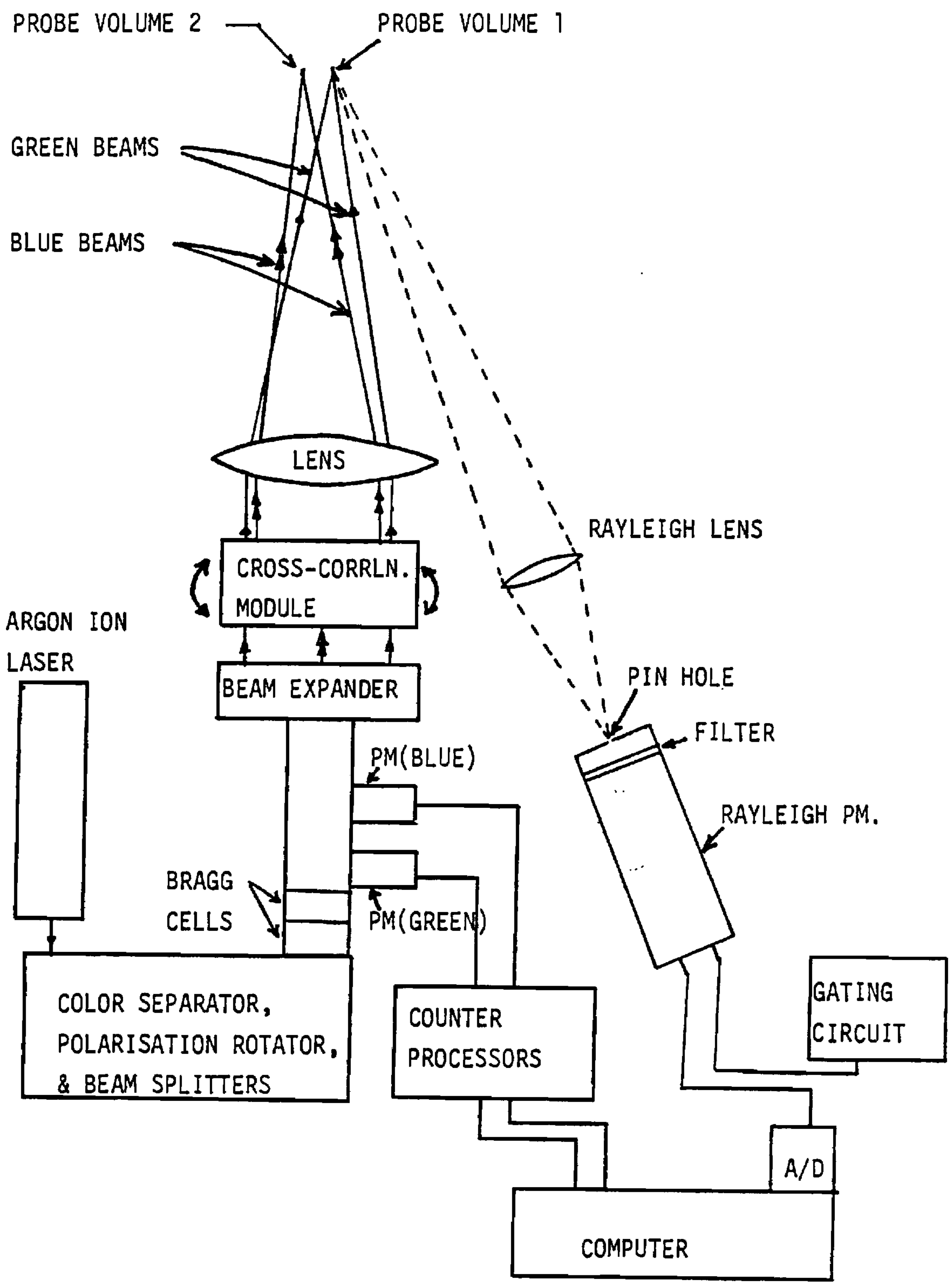

Figure 12. Instrumentation configuration for proposed work.

2. Measure the necessary space separated correlations to fully determine the pressure-velocity correlation
3. Compare against past intrusive measurements
4. Proceed to the pressure-strain, pressure-scalar and pressure-scalar gradient correlations presuming success on the pressure-velocity correlation.
5. Compare results on the pressure-strain and pressure scalar gradient correlations with the theory of Ref. (16) and modify the theory as necessary to bring theory and experiment into alignment.

Concerning the theory of Ref. (16), it was derived by making several approximations to Eq. (12). Consequently, using the proposed approach, a direct experimental check on those approximations will result. This approach will also shed some light on the constant density theory of Ref. (3) to the pressure-strain correlation.

It is to be emphasized that this program is not without risk. The primary risk element is the numerical sensitivity to the form of the experimental correlations. On the other hand, the approach almost guarantees that at least the magnitude of the results will be correct.

BIBLIOGRAPHY

1. Jones, W. P. (1980) Prediction Methods for Turbulent Flows (Kollmann, ed.) Hemisphere, 379.
2. Pope. S. B. (1981) Eighteenth Symposium (International) on Combustion, The Combustion Institute, 1001.
3. Launder, B. E., Reese, G. J. and Rodi, W. (1976) J. Fluid Mech. 68, 537.
4. Rotta, J. C. (1951) Z. Phys. 129, 547.
5. Lumley, J. L. (1975) Phys. Fluids 18, 750.

6. Lumley, J. L. (1975) Lecture Series No. 76, Von Karman Institute, Belgium.

7. Bray, K. N. C., Libby, P. A., Masuya, G. and Moss, J. B. (1981) Combust. Sci. and Technology 25, 127.

8. Kollmann, W. and Vandromme, D. (1979) AIAA Paper No. 79-1485.

9. Bilger, R. W. (1976) Prog. Energy Combust. Sci. 1, 87.

10. Starner, S. H. and Bilger, R. W. (1980) Combust. Sci. and Technology 21, 259.

11. Borghi, R. and Escudie, D. (1984) Combustion and Flame 56, 149.

12. Townsend, A. A. (1949) Aust. J. Sci. Res. 2, 451.

13. Kobashi, Y. (1957) J. Phys. Soc. Japan 12, 533.

14. Laufer, J. (1954) NACA Report 1174.

15. Starner S. H. and Bilger, R. W. (1987) Combust. Sci. and Technology, 53, 377.

16. Strahle, W. C. (1987) AIAA Paper No. 87-1351.

17. Komerath, N. M. and Strahle, W. C. (1983) AIAA Paper No. 83-0400.

18. Chandran, S. B. S., Komerath, N. M. and Strahle, W. C. (1985) Twentieth Symposium (International) on Combustion, The Combustion Institute, 429.

19. Waldherr, G. A., de Groot, W. A. and Strahle, W. C. (1988) submitted to Combustion and Flame.

20. Komerath, N. M., Hegde, U. G. and Strahle, W. C. (1983) AIAA Paper No. 83-0754.

21. McDaniel, J. C. (1983) AIAA Paper No. 83-0049.

22. Becker, H. A. and Brown, A. P. G. (1974) J. Fluid Mech. 62, 85.

23. Strahle, W. C. and de Groot, W. A. (1988) accepted in Combustion and Flame.

PRESSURE-DENSITY CORRELATION IN A TURBULENT REACTING FLOW

G. A. Waldherr , W. A. deGroot and W. C. Strahle

School of Aerospace Engineering

Georgia Institute of Technology

Atlanta, Georgia 30332, U.S.A.

PRESSURE-DENSITY CORRELATION IN A TURBULENT REACTING FLOW

Abstract

Progress toward extraction of the elusive pressure-density correlation in variable density reacting flows is reported upon in this paper, using a premixed methane–air flame in open surroundings as the test medium. The relationship between density and other scalars is shown. Molecular Rayleigh scattering, laser Doppler velocimetry, and dynamic Pitot barometry are the experimental techniques used. It is shown that the often neglected pressure–scalar correlation is an important quantity in scalar transport and must be taken into account theoretically in ways which differ from past treatment.

Introduction

In theoretical closure models for turbulent reacting flows, especially at the level of second order closure, correlations involving the pressure fluctuation have given extreme trouble to modelers [1]. Experimental information on such correlations is scant, if nonexistent, primarily because of the difficulty of obtaining static pressure fluctuation measurements and the current impossibility of making these measurements nonintrusively at the fluctuation level encountered in usual flows. Past progress has been made in measurement of pressure–velocity correlations in premixed [2,3] and diffusion flames [4] by either direct intrusive or indirect nonintrusive means, and the results have been quite illuminating. That is, many of the often made assumptions are simply incorrect and the pressure–velocity correlations play a large role in stress transport balance equations. The same may be expected of pressure–scalar correlations in scalar transport and these correlations are the subject of the current paper.

Of interest here are the correlations appearing in the vector D_i, where

$$D_i = \overline{c'' \frac{\partial p}{\partial x_i}} = \overline{c''} \frac{\partial \overline{p}}{\partial x_i} - \overline{p' \frac{\partial c''}{\partial x_i}} + \frac{\partial}{\partial x_i} \overline{p' c''} \tag{1}$$

In Eq. (1), p is pressure, c is any scalar, x_i is the i^{th} coordinate direction, an overbar indicates a conventional time average, a prime indicates a conventional fluctuation and a double prime indicates a mass–weighted (Favre) fluctuation. The first term on the right side of Eq. (1), where $\overline{c''} = -\overline{\rho' c'}/\overline{\rho}$ and ρ is density, usually gives no trouble (it will, in fact, be zero in the flame considered here because of near zero mean pressure gradient) and is of no concern in this paper. The second term is called the pressure–scalar gradient correlation and the differentiated quantity, $\overline{p'c''}$, in the third term is called the pressure–scalar correlation. It is this term which is of primary concern in this paper. The pressure–scalar correlation is usually either neglected or incorporated into a diffusion term [5] in scalar transport equations, a practice which will be shown in this paper to be unwise.

Theory

Some idea of what is to be expected from the correlation of interest may be obtained by viewing an approximate solution for the pressure fluctuation for a flow in an unbounded medium [for full explanation of the approximations involved, see Ref. 6].

$$p'(x_i,t) = \int dV(y_i)\; G(x_i,y_i) \frac{\partial^2(\overline{\rho}\,\tilde{v}_\ell v''_m)}{\partial y_\ell \partial y_m} \qquad (2)$$

Here V is the volume of all space, v_ℓ is the velocity in the ℓ^{th} direction, y_i is the space variable of integration, a tilda denotes a mass–weighted average and G is the free space Green's function, $(|\,(x_i-y_i)(x_i-y_i)\,|^{1/2}\,4\pi)^{-1}$. The correlation in question is given by multiplication of Eq. (2) by $c''(x_i,t)$ and time averaging, producing a two point, space separated correlation and its derivatives under the integral. The double derivative in the integral, being a double divergence, produces many non–negligible terms. While each term may be of the order of magnitude of $\overline{\rho}\,\tilde{v}\,\overline{c''v''}$, the number of terms leaves the expected magnitude uncertain. With no theory for guidance, measurement seems the only resource for help, if the measurement may be reliably made.

The scalar may be quantities like temperature, mass fraction, or, as is the case here, ρ'/ρ which appears in the transport equation for the density-velocity covariance [1]. This covariance will be approximated, as is usual, by $\overline{v''_i\rho'/\rho} \simeq \overline{\rho' v''_i}/\overline{\rho}$; the approximation yields analytical simplification which, while not numerically exact, should yield adequate semi–quantitative and certainly qualitative results in highly variable density flows. It should be noted here that a peculiarity of mass–weighted averaging yields exactly $\overline{\rho' v''_i} = \overline{\rho' v'_i}$. From intrusive measurement [2,3] on the axis of an axisymmetric turbulent flame it is known that $\overline{\rho' v'_i}$ should be of the order of magnitude of $0.01\overline{\rho}\,\overline{v}_1$, where the 1 subscript denotes the axial direction. This order of magnitude is small, however, it will be shown to actually aid the confidence with which the pressure–scalar correlation may be determined.

By way of theoretical confirmation, along the axis of a premixed turbulent flame in open surroundings, where experimentally [3] $\overline{v}_1$ is approximately constant, the following differential equation may be derived for the density–velocity covariance:

$$\tilde{v}_j \, \overline{\rho} \frac{\partial}{\partial x_j} (\overline{\rho' v_i''}) - \overline{\rho' v_i''} \, \tilde{v}_j \frac{\partial \overline{\rho}}{\partial x_j} = -\overline{v_j''^2} \, \overline{\rho} \frac{\partial \overline{\rho}}{\partial x_i} + K \, \overline{\rho' v_i''} \, \tilde{v}_j \frac{\partial \overline{\rho}}{\partial x_j} \tag{3}$$

In Eq. (3) theory has been used for the pressure–scalar gradient correlation with K=0 using the theory of Ref. 1 and K=0.6 for the theory of Ref. 6. By *a posteriori* inspection of magnitudes diffusion has been neglected in Eq. (3), and the pressure–scalar correlation has been neglected. Using the continuity equation $\partial(\overline{\rho}\, \tilde{v}_i)/\partial x_i = 0$, and assuming for order of magnitude estimates that $\tilde{v}_i \approx \overline{v}_i$, Eq. (3) may be integrated along the axis to yield

$$\overline{\rho' v_i'} = \frac{\overline{\rho}\, \overline{v_i''^2}}{\overline{v}_1 K} \left[1 - \left(\frac{\overline{\rho}}{\overline{\rho}_o} \right)^K \right] \tag{4}$$

where $\overline{\rho}_o$ is the cold gas density. Equation (4) also shows the above expected order of magnitude for this correlation if $| v_1'/\overline{v}_1 | \approx 0.1$ (as it is) and the behavior of the correlation is as measured in Ref. 3.

Apparatus

The Burner

The burner and premixed flame are shown in Fig. 1. A stoichiometric mixture of methane and air flows through the mouth of a brass burner of inner diameter 2.54cm. The turbulent premixed flame is anchored to the burner by a small annular methane diffusion flame approximately 0.7cm long. The methane–air mixture flows through a long pipe of 30 pipe diameters and exits the burner with a Reynolds number of 10000. The velocity profile at the exit was verified experimentally to be turbulent and fully developed. The flame is vertical and is surrounded by a 1.8m × 1.8m enclosure with the exhaust products vented at least thirty diameters above the burner exit. The entire burner assembly is mounted on a traversing platform to allow property measurement at different locations within the flame.

Velocity Measurement

The axial velocity of the jet was measured nonintrusively using one component of a 5W two–component argon–ion laser Doppler velocimeter operating in back–scatter mode. By crossing two beams of the same color (in this case, the green beams at 514nm) an interference pattern is generated. A particle crossing the fringes created by this interference will scatter the laser light giving a sinusoidally varying signal whose frequency is inversely proportional to the velocity. This signal is collected by a photomultiplier and then processed by a counter which measures the frequency by determining the time necessary to complete a fixed number of cycles. The velocity and time of arrival information is available digitally as an output from this counter.

The premixed flow was seeded with titanium dioxide particles with a nominal diameter of 1 micron. A fluidized bed aerosol generator introduced the particles to the flow far upstream of the burner, so that the mixture was seeded uniformly.

Pressure Measurement

A specially constructed microphone Pitot probe shown in Fig. 2 is used within the flame. The tip of the probe consists of a 2.54cm long ceramic tube with outside diameter 1.6mm and inside diameter 0.8mm because this was the smallest diameter tip that did not attenuate the signal below the threshhold of the microphone. This configuration displayed a sensitivity of about 0.1Pa and the largest fluctuations expected were of the order of 50Pa. The portion of the probe behind the ceramic tube is covered by a water–cooled jacket which, along with the ceramic tip, help to avoid flameholding of the probe. The entire tube is situated ahead of a Brüel & Kjær 1.27cm condenser microphone and preamplifier.

The Pitot tube causes the flow to stagnate in a small region near the probe tip.

The arrangement above has been shown to measure the instantaneous total pressure that would exist at the probe tip in the absence of the probe [3]. A Pitot tube also measures the total pressure well for angles of attack up to 10 degrees [7]. The axial velocity pdf shown in Fig. 3 is one of the broadest pdfs found along the flame axis, and the high concentration of velocities about the mean shows that the fluctuating component is less than 20% of the mean axial velocity. Since, within a free jet, the transverse velocity is zero along the axis, this indicates that the angle of attack of the flow is within the limits specified previously.

The total pressure is a function of static pressure, density, and velocity. Simultaneous measurement of the density and velocity near the tip allows the recovery of the instantaneous static pressure at the probe tip. Under a locally quasi–steady assumption for the stagnation process, the total pressure p_t in low speed flows is

$$p_t = p + \frac{1}{2}\rho v^2 \tag{5}$$

Reynolds decomposition is performed on Eq. (5) and a subsequent experimental order–of–magnitude analysis [2] shows that the approximate relation between fluctuations in total pressure, static pressure, density, and velocity is

$$p_t' = p' + \bar{\rho}\,\overline{V}\,v' + \frac{1}{2}\rho'\,\overline{V}^2 \tag{6}$$

where $\bar{\rho}$ and $\overline{V}$ denote the mean density and the mean axial velocity.

To allow for the varied response of the probe within the flame, a calibration was performed to compensate the microphone signal in both amplitude and phase over the frequency range of interest. The signal from the Pitot microphone was compared to a reference microphone and a complex transfer function was computed. A simultaneously computed coherence function near unity ensured validity of the transfer function. The calibration was performed at various temperatures to allow for the effect of heating on, and hence sound speed, density, and viscosity changes within, the ceramic tip. The water–cooled jacket maintained the remainder of the probe at the ambient temperature.

Density Measurement

To facilitate the measurement of density, one component of the laser was used as the source for Rayleigh scattering of light off of the molecules within the flame. The light scattered by the molecules crossing within the probe volume was collected by a lens and subsequently passed through slits, focusing lenses, and a polarizing filter, and sensed by a photomultiplier. From the theory of Rayleigh scattering a relation between the scattering intensity, density, and scattering cross–section is [8]

$$I_s = K \rho \, (d\sigma/d\Omega)_{eff} \tag{7}$$

where I_s is the scattered intensity, K is a calibration factor, ρ is the density, and $(d\sigma/d\Omega)_{eff}$ is the effective scattering cross–section. Equation (7) shows the signal from the photomultiplier is proportional to the density of the fluid in the probe volume and, therefore, dependent on the molecules within the probe volume. For methane–air combustion the problem of different molecules within the volume is avoided because the average molecular weight of the reactants is nearly the same as the average molecular weight of the products and the scattering cross–section of the methane-air mixture nearly matches the scattering cross–section of the product gases. Also, using the assumption of a single–step irreversible chemical reaction to conform to Bray–Moss–Libby structure [9,10], only reactants or products can be dominantly present at any point in the flow. One reason for using a stoichiometric flame was to closely achieve this structure, which was not achieved in Ref. 3. The proportionality between density and scattering intensity is therefore a constant and was determined from a calibration using a stoichiometric nonreacting methane–air mixture at ambient temperature for reference.

The density was chosen as the scalar of interest because it is the simplest to measure and the density can also be related to the progress variable c. Using relations from Ref. 11, the progress variable can be shown to be an inverse function of the density, namely

$$c = \frac{K_1}{\rho} - K_2 \tag{8}$$

where

$$K_1 = \frac{\overline{p}/R}{T_\infty - T_\circ} \qquad K_2 = \frac{T_\circ}{T_\infty - T_\circ}$$

Here, R is the universal gas constant, T_∞ is the temperature of the products (adiabatic flame temperature), and $T_\circ$ is the ambient temperature. In a turbulent jet the mean pressure can be assumed to be constant, resulting in K_1 and K_2 being constant. From Eq. (8) the mass–weighted fluctuation c'' is found to be

$$c'' = \frac{K_1}{\overline{\rho}} \left(\frac{\rho'}{\rho}\right) \tag{9}$$

In comparison with the density measurement the background noise present in the c'' measurement is more difficult to decouple from the true measurement because of the ratio of two fluctuating quantities, ρ' and ρ.

Data Acquisition

For the measurement of the total pressure–density correlation the pressure probe measurement volume and the laser probe volume were aligned to get the closest spacing permissible for which each measurement would not be affected by interference from the other. The resulting separation between measuring points became 3mm. The laser light had virtually no effect upon the pressure sensed by the Pitot probe. The ceramic tip of the Pitot tube however reflected some of the laser light causing changes in the density measured. The separation distance was adjusted until the Pitot probe just began to influence the density, at which point the Pitot probe was backed away slightly.

The signals from the Pitot probe and the photomultiplier were then sent through amplifiers and filters and finally sampled by a Preston 14–bit A/D converter and an HP1000 minicomputer system. The photomultiplier signal was filtered to eliminate the high-frequency spikes caused by occasional particles within the probe volume. The pressure signal was filtered to reduce the frequency components of the signal above the highest frequency of interest. Each of the signals was sampled at least 5000 times at a rate of 3000Hz which is more than twice the highest frequency component of interest. The entire time–series were temporarily stored in the volatile memory of the computer and processed into power spectra or pdfs before storage.

To measure the density–velocity correlation a compromise between the conflicting requirements of seeded flow for the velocimeter and clean flow for the Rayleigh scattering was necessary. The counter from the velocimeter was directly linked to the computer through one of the external ports. Special in–house software was used to buffer the data coming through the A/D converter from the Rayleigh scattering until a signal was received from the counter that a valid velocity point was acquired. At this time the density data from the A/D converter was recalled and stored along with the data from the counter. This arrangement allowed the measurement of density at 20 points before and after a valid velocity point. The density data was then further processed to remove the peak caused by the particle saturating the photomultiplier as it crossed the probe volume. To these ends the seeding rate had to be decreased to allow the measurement of the density between the velocity points. Data acquisition rates of approximately 5 samples per second were achieved by this method.

Data Reduction Techniques

For the verification of bimodality within the flame the density signal was converted from a time–series to a pdf. The bimodality was investigated since its existence is an indication of Bray–Moss–Libby theoretical structure. Simply converting the density signal to a pdf was not sufficient because of a significant amount of background noise from the natural luminosity of the flame. This background noise was recorded for every measurement with the laser off. To remove the background noise of the flame a deconvolution of the background noise and the combined true density with background pdf was performed [12]. The true density pdf within the flame was thus recovered. The pressure signal was not necessary to determine bimodality.

During measurement of the pressure–density correlation the two signals were converted from the time–domain to the frequency–domain via Fourier transforms. The transforms were processed into autospectra and a complex cross–spectrum and stored on magnetic media. The autospectrum and cross–spectrum were then converted via inverse Fourier transforms into autocorrelations and a cross–correlation [13]. As in the bimodality measurements the background noise was significant and the correlations were recorded both with the laser on and the laser off. The true correlations could then be determined by subtracting respective cross–correlations and under the assumption that the noise is uncorrelated with the true density the true autocorrelations could be determined by addition.

During measurement of the density–velocity correlation the two signals were converted to pdfs. The background noise again had to be removed by a deconvolution process similar to the one used to determine the true density pdf for bimodality. The background noise in the density signal was assumed to be uncorrelated with the velocity. This fact, along with the slender profile of the velocity pdf, allowed the joint density–velocity pdf to be deconvoluted using the background density and the average velocity.

Taking Eq. (6) and multiplying throughout by ρ' and then time–averaging, results in the working relation

$$\overline{p'\rho'} = \overline{p_t'\rho'} - \bar{\rho}\,\overline{V}\,\overline{\rho' v'} - \frac{1}{2}\overline{V}^2\,\overline{\rho'^2} \tag{10}$$

From Eq. (10) it can be seen that the static pressure–density correlation could be determined from knowledge of the total pressure–density correlation, density–velocity correlation, and density autocorrelation and also the mean density and velocity. One advantage that arises from the expansion shown in Eq. (10) is the ability to independently determine each correlation in separate experiments. Each of the correlations is statistically valid since a large number of samples was used to determine the correlation. The largest values of the correlations were then used to calculate the static pressure–density correlation.

Results

The flame is shown schematically in Fig. 1. It consists of a cold inner core of reactants surrounded by a very luminous reaction zone, above which is a large region of low luminosity product gases. The reaction zone converges about 2.3 diameters from the burner mouth and extends to a distance of about 2.8 diameters downstream. The temperature in the inner core approaches the ambient temperature towards the mouth of the burner and the temperature in the product region approaches the adiabatic flame temperature of 2250K for a stoichiometric methane–air reaction.

The region of most intense reaction appears at about 2.4 diameters downstream and it is at this point that the probability distribution is most nearly bimodal. The evolution of the probability distribution along the centerline of the flame is presented in Fig. 4. The bimodal distributions are a result of the flame front oscillating about the probe volume. The distributions have very smooth and broad profiles due to the deconvolution process which was necessary to remove the background noise from the true signal. Figure 4 shows that the Bray–Moss–Libby theoretical structure [9,10] is indicated by the flame and resulting simplifications from that theory can be applied to further invesigations.

A representative density autospectrum is shown in Fig. 5. The low signal level above 1000Hz shows that the important information within the signal occurs below 1000Hz. The frequency components through 1500Hz were always sampled to ensure that all the signals decayed by that point.

Axial profiles of the terms comprising the largest static pressure–density correlation are shown in Fig. 6. From these profiles it can be seen that the total pressure–density correlation and the density autocorrelation terms are the main contributors to the static pressure–density correlation. The density–velocity correlation term, even though the most uncertain of the three correlations, is negligible in comparison with the others. The static pressure–density correlations were computed from the terms shown in Fig. 6 and the resulting axial profiles is shown in Fig. 7 along with the error bounds of the calculation. The error bounds were determined from the statistical deviation of the separate correlations. These deviations were determined by repeating the experiments at later dates and finding the standard deviation from the average of these separate measurements. The error bounds in the figure are a result of the subtraction of terms with the same order of magnitude and experimental error in the determination of the correlations.

From Fig. 7 it can be seen that the pressure–density correlation decreases, and later increases, by 0.3 Pa·kg/m^3 within half a pipe diameter, yielding a gradient whose magnitude is about 25 Pa·kg/m^4. For the same flame, the largest term in Eq. (3) has a magnitude of about 5 Pa·kg/m^4 within the flame. Also, the density–velocity correlation must be zero when exiting the burner and must decay to zero far downstream of the flame. From these results it can be seen that the pressure–scalar correlation can not be neglected. The overall effect of the pressure–scalar correlation, however, will be negligible if the entire flame is considered, since the pressure–scalar correlation is a dominating term only in the vicinity of the flame.

Conclusions

1. The pressure–scalar correlation is not a negligible quantity in turbulent flames and is important in the scalar transport balance equations.
2. The density–velocity correlation is not significant in pressure–density correlation determination.
3. Interestingly, the structure of this turbulent premixed flame is approximated well by Bray–Moss–Libby theory. This was not necessary for the current data analysis but may prove useful in future analyses.

Acknowledgements

This work was supported by the National Science Foundation under Grant No. CBT-8414906. Useful discussions with Prof. N. M. Komerath are gratefully acknowledged.

References

1 Jones, W. P., in *Prediction Methods for Turbulent Flows* (Kollman ed.). Hemisphere, 1980, p. 379.

2 Komerath, N. M. and Strahle, W. C. *Measurement of the Pressure–Velocity Correlation in Turbulent Reactive Flows.* Paper 83-0400, AIAA Twenty–first Aerospace Science Meeting, Reno, NV (1983).

3 Chandran, S. B. S., Komerath, N. M. and Strahle, W. C. *Twentieth Symposium (International) on Combustion.* Combustion Institute, 1984, p.429.

4 Starner, S. H. and Bilger, R. W. *Comb. Sci. and Tech.* 53:377 (1987).

5 Launder, B. E., in *Turbulence* (Bradshaw ed.). Springer–Verlag, 1978, p. 232.

6 Strahle, W. C. *Pressure–Strain and Pressure–Scalar Gradient Correlation in Variable Density Turbulent Flows.* Paper 87-1351, AIAA Nineteenth Fluid Dynamics Conference, Honolulu, HI (1987); accepted AIAA Journal.

7 Becker, H. A. and Brown, A. P. G. *J. Fluid Mech.* 62:85 (1974).

8 Dibble, R. W. and Hollenbach, R. E. *Eighteenth Symposium (International) on Combustion.* Combustion Institute, 1981, p. 1489.

9 Bray, K. N. C. and Moss, J. B. *Acta Astronautica* 4:291 (1977).

10 Libby, P. A. and Bray, K. N. C. *Comb. Flame* 39:33 (1980).

11 Bray, K. N. C., in *Turbulent Reacting Flows* (Libby and Williams ed.). Springer–Verlag, 1980, p. 141.

12 Strahle, W. C. and deGroot, W. A. *Comb. Flame* 74:193 (1988).

13 Bendat, J. S. and Piersol, A. G. *Engineering Applications of Correlation and Spectral Analysis.* Wiley–Interscience, 1980, p. 1.

Figure Captions

Figure 1. Geometry of the burner and the flame.

Figure 2. a. Microphone Pitot probe configuration. b. Data acquisition system.

Figure 3. A velocity pdf within the flame with one of the broadest profiles.

Figure 4. Evolution of the density probability distribution function along the centerline of the flame.

Figure 5. A characteristic density autospectrum.

Figure 6. Centerline axial profiles of the various terms comprising the static pressure–density correlation, namely, (a) the total pressure–density correlation, (b) the density–velocity correlation term, and (c) the density autocorrelation term.

Figure 7. Axial profile of the static pressure–density correlation along the centerline of the flame, including error bounds.

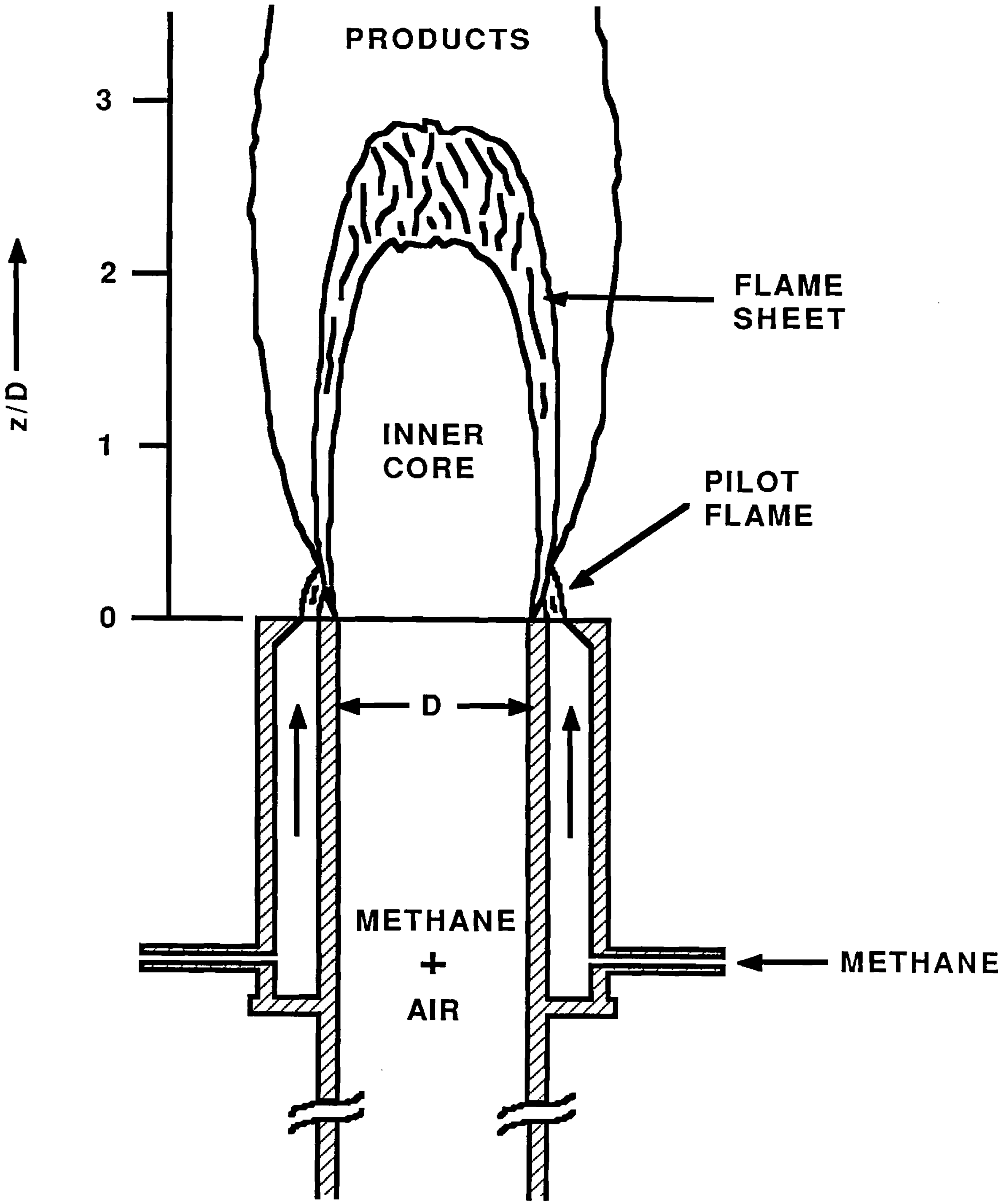

PRODUCTS
3
2
1
0
z/D
FLAME
SHEET
INNER
CORE
PILOT
FLAME
D
METHANE
+
AIR
METHANE

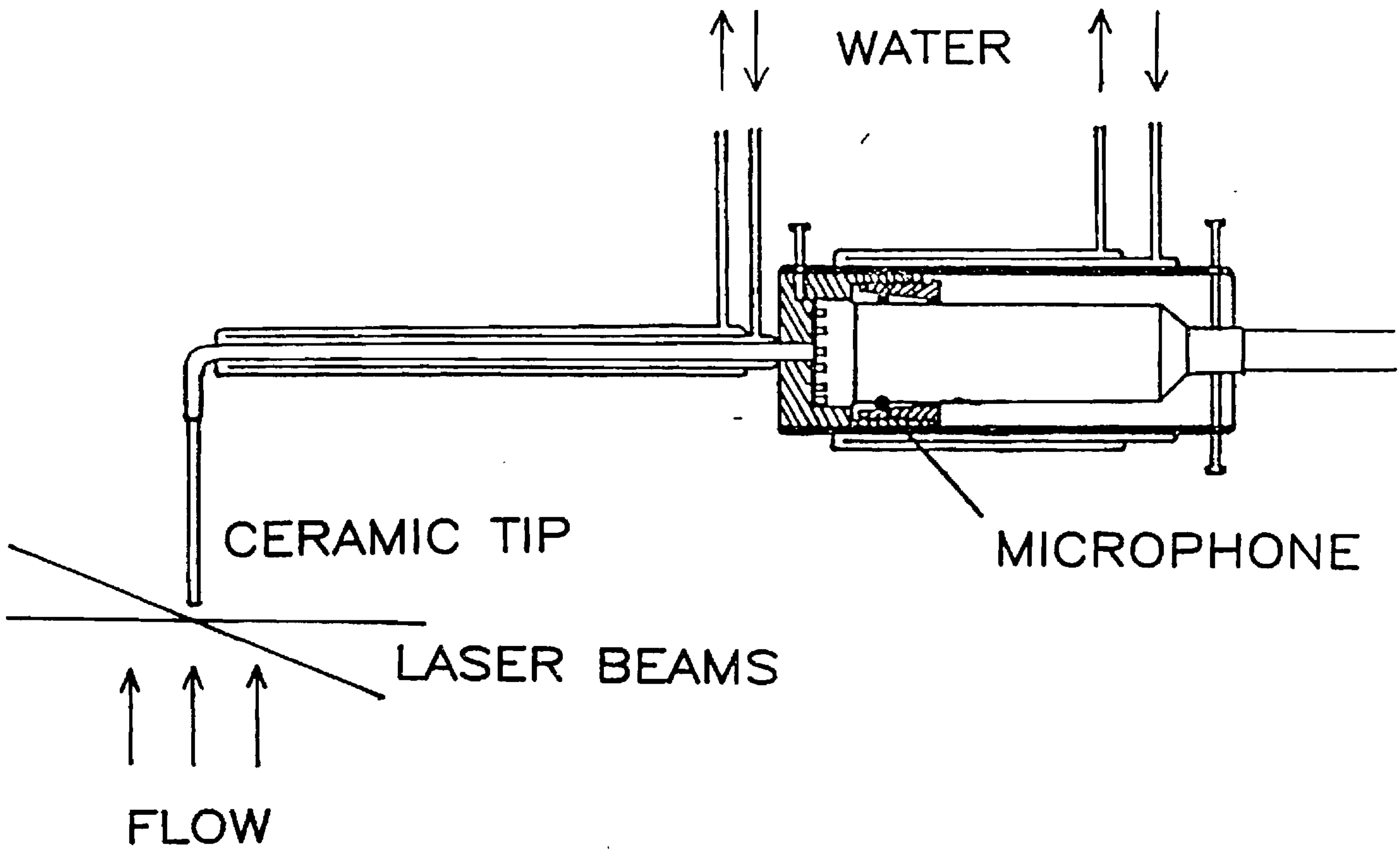
WATER
CERAMIC TIP
MICROPHONE
LASER BEAMS
FLOW

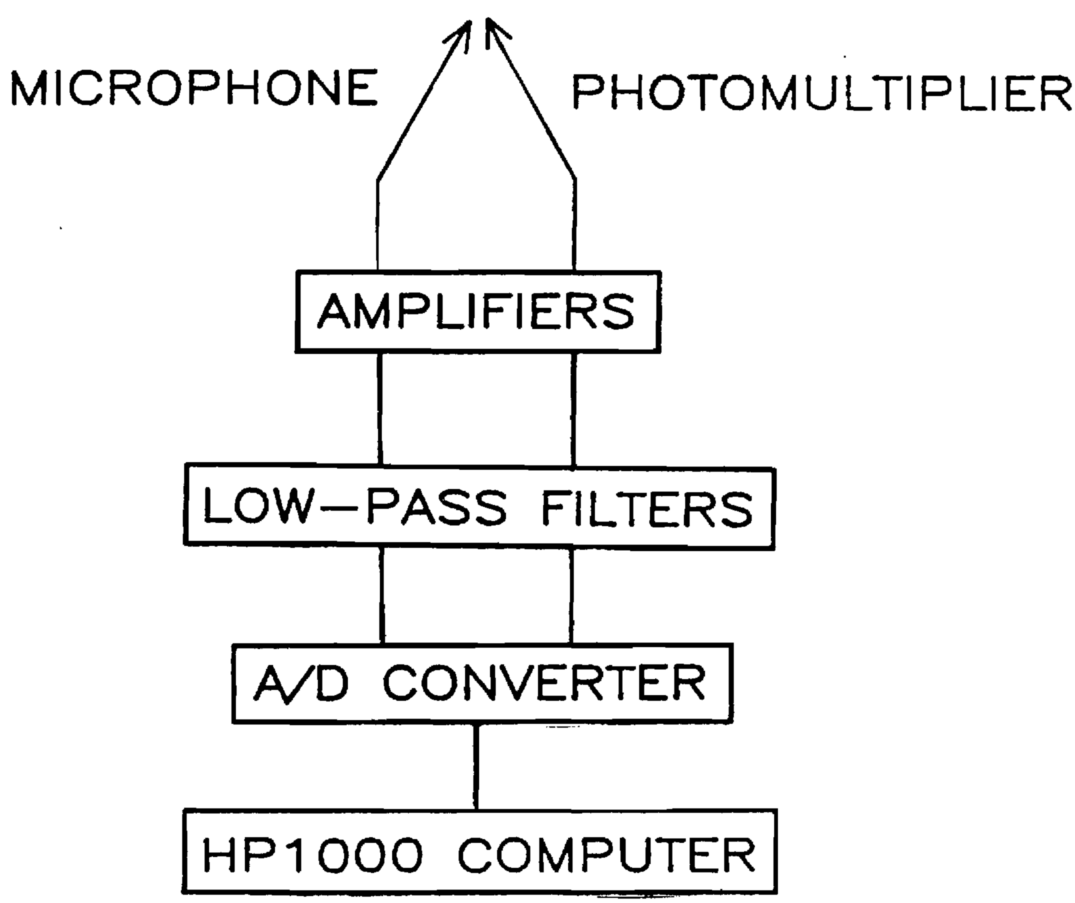
MICROPHONE
PHOTOMULTIPLIER
AMPLIFIERS
LOW-PASS FILTERS
A/D CONVERTER
HP1000 COMPUTER

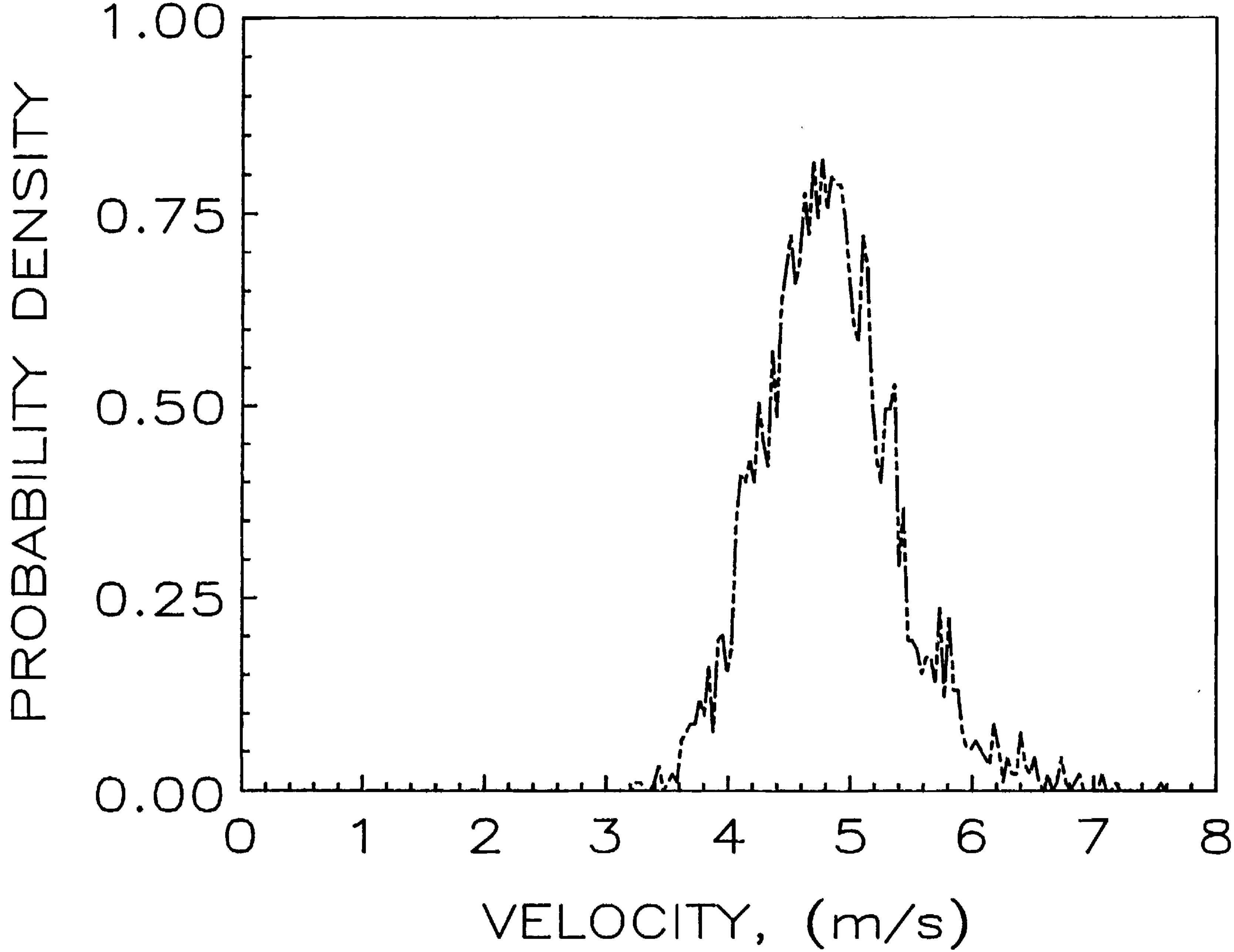
PROBABILITY DENSITY
1.00
0.75
0.50
0.25
0.00
0
1
2
3
4
5
6
7
8
VELOCITY, (m/s)

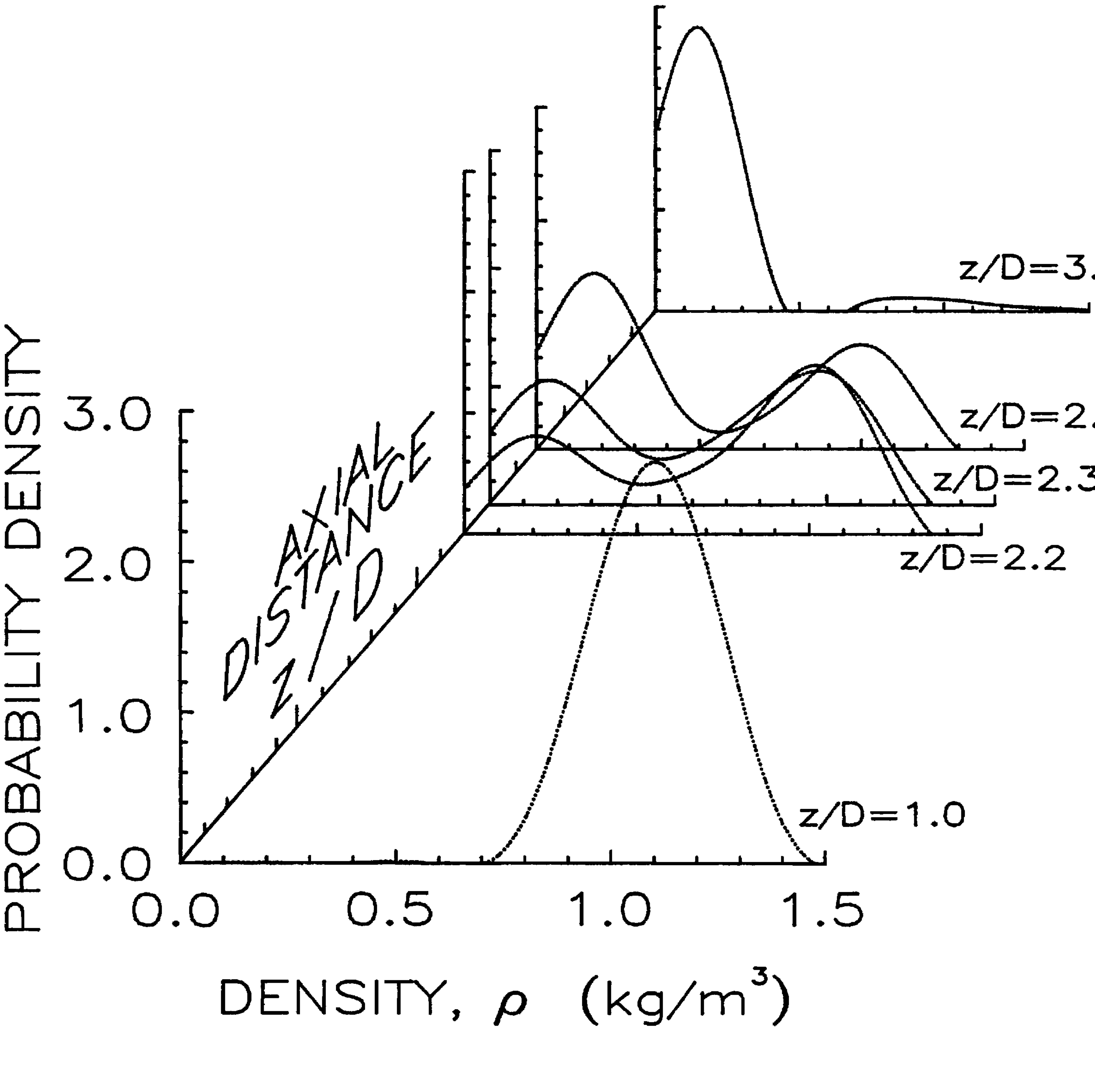

PROBABILITY DENSITY
3.0
2.0
1.0
0.0
0.0
0.5
1.0
1.5
DENSITY, ρ (kg/m³)
AXIAL DISTANCE Z / D
z/D=3.
z/D=2.
z/D=2.3
z/D=2.2
z/D=1.0

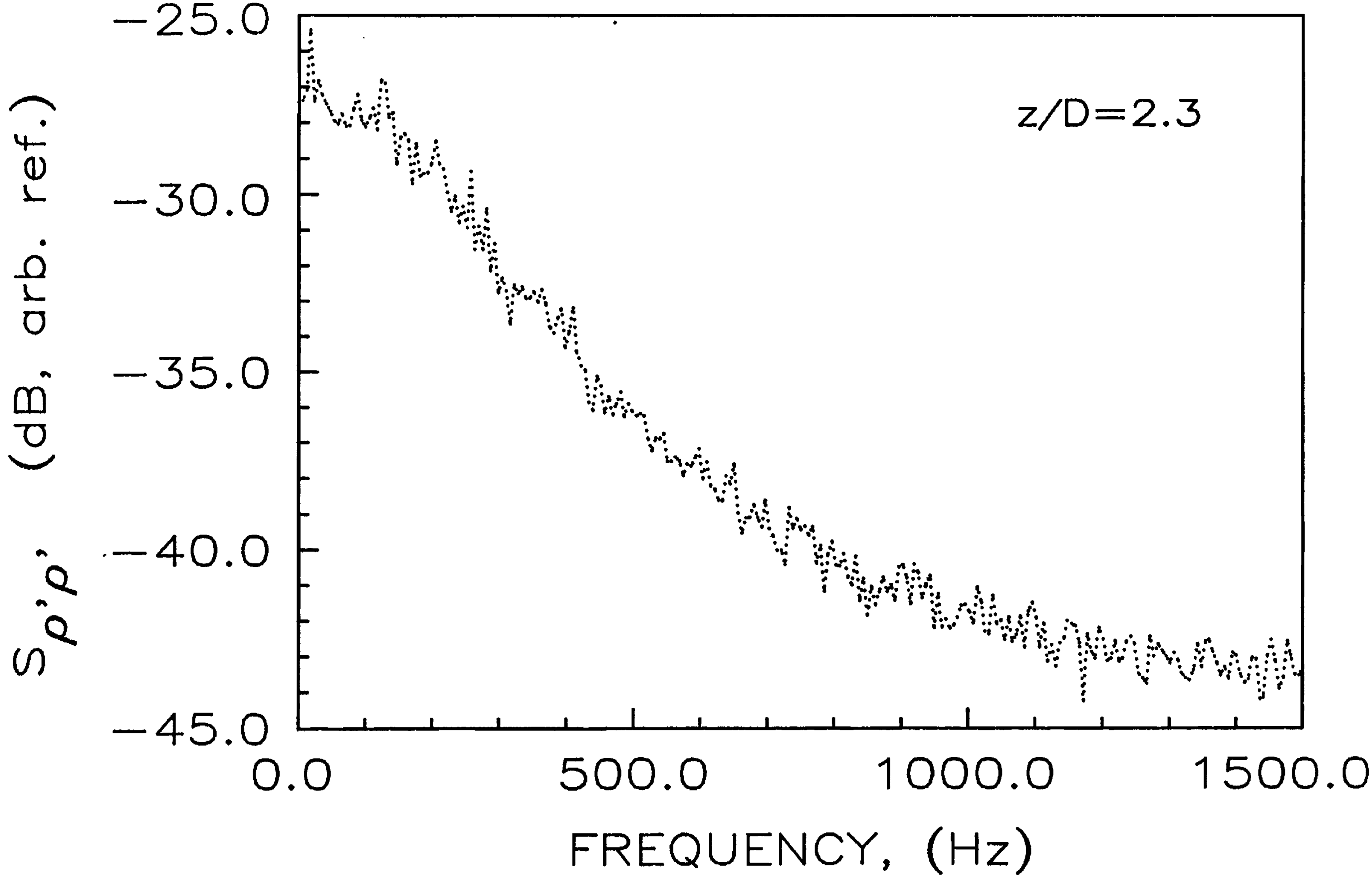

-25.0
-30.0
-35.0
-40.0
-45.0
S ρ'ρ' (dB, arb. ref.)
z/D=2.3
0.0
500.0
1000.0
1500.0
FREQUENCY, (Hz)

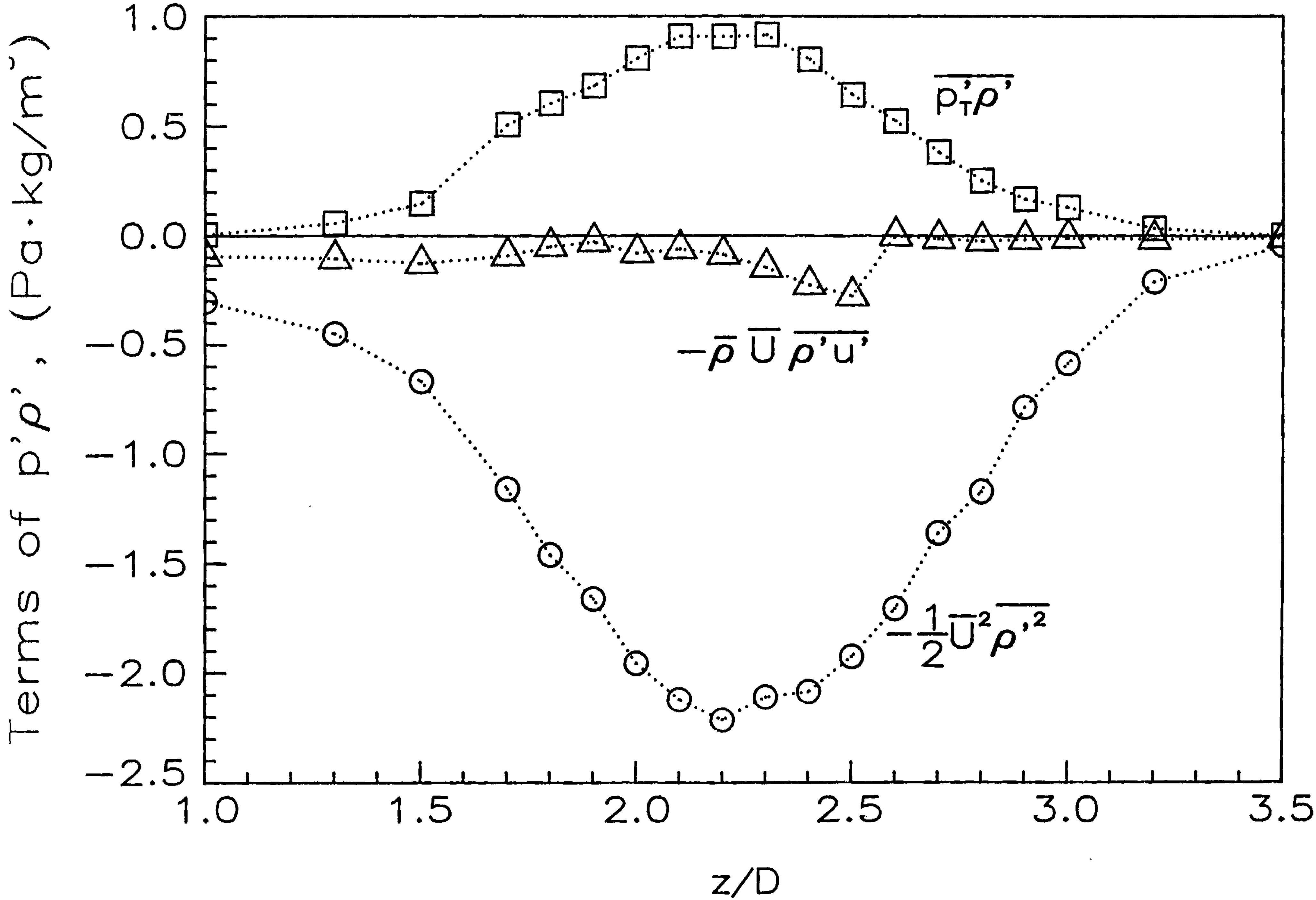

Terms of p'ρ' , (Pa·kg/m³)
1.0
0.5
0.0
−0.5
−1.0
−1.5
−2.0
−2.5
1.0
1.5
2.0
2.5
3.0
3.5
z/D
$\overline{p_T'\rho'}$
$-\bar{\rho}\,\overline{U}\,\overline{\rho' u'}$
$-\frac{1}{2}\overline{U}^2\overline{\rho'^2}$

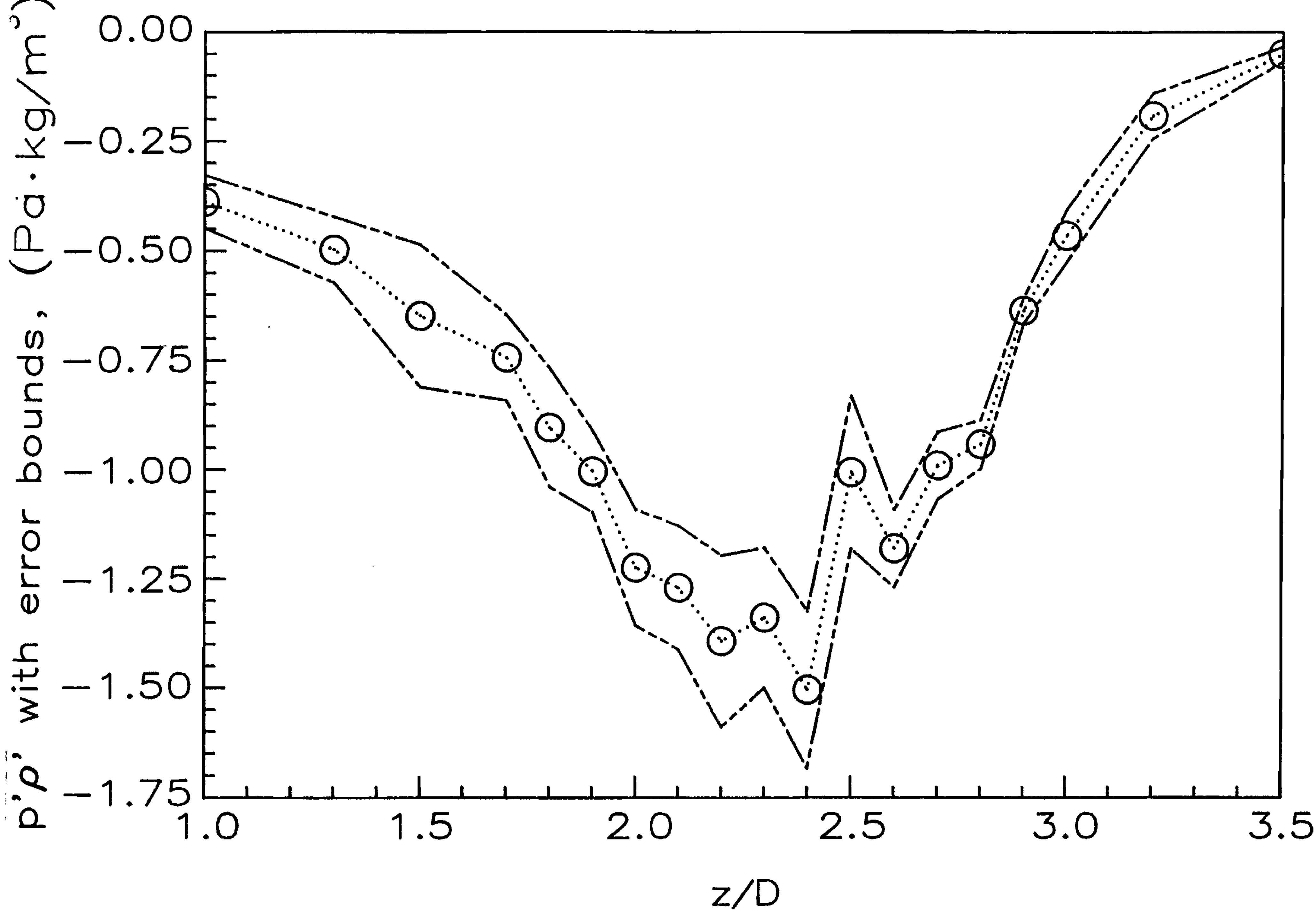
p'ρ' with error bounds, (Pa·kg/m³)
0.00
−0.25
−0.50
−0.75
−1.00
−1.25
−1.50
−1.75
1.0
1.5
2.0
2.5
3.0
3.5
z/D